Dipl.-Ing. Norbert Essl

Dynamic Behavior of Synchronous Machines Relating to LVRT Requirements

DOCTORAL THESIS

to achieve the university degree of

Doktor der technischen Wissenschaften

submitted to

Graz University of Technology

Supervisor

Ao.Univ.-Prof. Herwig Renner

Institute of Electrical Power Systems

Prof. Emmanuel De Jaeger
Ecole Polytechnique de Louvain

Graz, December 2016

Affidavit

I declare that I have authored this thesis independently, that I have not used other than the declared sources/resources, and that I have explicitly indicated all material which has been quoted either literally or by content from the sources used. The text document uploaded to TUGRAZonline is identical to the present doctoral thesis.

Date	Signature

Table of Contents

i. List of Abbreviations

AEE	Asociación Empresarial Eólica
AVR	Automatic Voltage Regulator
BDEW	Bundesverband der Energie- und Wasserwirtschaft
CEA	Canadian Electrical Association
CEER	Coucil of European Energy Regulators
CIGRE	Conseil International des Grands Réseaux Electriques
DFIG	Doubly-Fed Induction Generator
DSO	Distribution System Operator
EMT	Electro-magnetic transients
ENTSO-E	European Network of Transmission System Operators of Electricity
EPRI	Electric Power Research Institute
EUT	Equipment under test
FGW	Fördergesellschaft Windenergie und andere Erneuerbare Energien
FRT	Fault-ride-through
HV	High voltage
HVRT	High-voltage-ride-through
IEC	International Electrotechnical Commission
LV	Low Voltage
LVRT	Low-voltage-ride-through
MV	Medium voltage
NPL	National Power Laboratory
OLTC	On-load tap changer
PCC	Point of common coupling
PGU	Power generation unit
RMS	Root mean square
SCR	Short circuit ratio
TSO	Transmission System Operator
VRT	Voltage Ride Through
WECC	Western Electricity Coordinating Council

ii. List of Symbols

α	Reciprocal value of armature time constant τ_a
ϑ	Rotor angle
τ_a	Armature time constant
Ψ_d	Flux linkage d-axis
Ψ_q	Flux linkage q-axis
ω	Angular frequency
ω_0	Angular frequency at rated speed
ω_n	Natural angular frequency
CF	Correction Factor
E'	Voltage behind transient reactance X_d'
E_B	Voltage at point B of external grid
E_{FD}	Exciter output voltage
F_{EX}	Rectifier loading factor
H	Inertia time constant
I_0	Transformer no-load current
i_{d0}, i_{q0}	Steady state instantaneous d/q-axis current
i_{dt}, i_{qt}	Decaying exponential component of d/q-axis current
I_{FD}	Field current
I_{SC}	Short circuit current
K_A	Voltage regulator gain
K_D	Demagnetizing factor
K_{DR}	Voltage regulator derivative gain
K_E	Exciter constant
K_{IR}	Voltage regulator integral gain
K_{PR}	Voltage regulator proportional gain
K_S	Synchronizing torque
L_{1d}	Damper winding leakage inductance
L_{ad}, L_{aq}	Stator to rotor mutual inductance in d/q-axis
L_d, L_q	Synchronous inductance in d/q-axis
L_{fd}	Field winding leakage inductance
L_l	Stator leakage inductance
P_{BS}	Retarding power due to backswing effect
P_{cu}	Transformer copper losses
P_D	Damping power

pf	Power factor
P_{gen}	Generator electrical power output
P_{Load}	Machine loading
P_{r}	Rated active power
P_{T}	Turbine power
P_{V}	Dissipated power
r_{a}	Armature winding resistance
R_{d1}, R_{d2}, R_{q}	Damper and field winding resistances[1]
R_{S}	Series resistance
S_{E}	Exciter saturation function
S_{Fault}	Short circuit power at fault location
S_{k}"	Short circuit power
S_{n}	Nominal apparent power
S_{PCC}	Short circuit power at PCC
T_{A}	Voltage regulator time constant
T_{d}', T_{q}'	Transient short circuit d/q-axis time constant
T_{d}", T_{q}"	Sub-transient short circuit d/q-axis time constant
T_{DR}	PID lag time constant
T_{e}	Electrical torque
T_{E}	Exciter time constant
t_{f}	Fault duration
u_{k}	Transformer short circuit voltage
U_{n}	Nominal voltage
U_{n1}, U_{n2}	Transformer primary/secondary nominal voltage
U_{ret}	Remaining voltage at fault location
ut	Terminal voltage
v_{d0}, v_{q0}	Steady state instantaneous d/q-axis voltage
V_{E}	Exciter voltage back of commutating reactance
V_{EMIN}	Minimum exciter voltage output
V_{FEMAX}	Exciter field current limit
V_{REF}	Reference voltage
V_{RMIN}, V_{RMAX}	Maximum/minimum voltage regulator output
V_{S}	Stator voltage
V_{X}	Signal proportional to exciter saturation

[1] Calculations see [1]

x_c	Connection impedance
x_d, x_q	Synchronous d/q-axis reactance
x_{du}	Unsaturated d-axis reactance
x_d', x_q'	Transient d/q-axis reactance
x_d", x_q"	Sub-transient d/q-axis reactance
x_T	Total impedance
Z_1	LVRT test container series impedance
Z_2	LVRT test container shunt impedance
Z_F	Fault impedance
Z_S	Source impedance

iii. List of Publications during PhD thesis work

1. N. Essl and H. Renner, "Modellierung und Validierung von LVRT-Simulationsmodellen Dezentraler Erzeugungseinheiten", in *13. Symposium Energieinnovation,* Graz, Technische Universität Graz, 2014.
2. N. Essl and H. Renner, "LVRT-Retardation-Device for Decentralized Power Plants", in *2014 Electric Power Quality and Supply Reliability Conference PQ2014*, *IEEE Proceedings*, Rakvere, 2014.
3. N. Essl and H. Renner, "Low-Voltage-Ride-Through-Assistenzsystem für dezentrale Erzeugungseinheiten", in *e&i Elektrotechnik und Informationstechnik*, Springer Verlag, Wien, 2014.
4. N. Essl and H. Renner, "Influence of LVRT Test Equipment Characteristics on the Dynamic Performance of a Power Generation Unit", in *23rd International Conference on Electricity Distribution (CIRED)*, Paper 1133, Lyon, 2015.
5. N. Essl and H. Renner, "Assessing the Severity of Voltage Sags Due to Short Circuits in Transmission and Distribution Grids", in *17th International Conference on Harmonics and Quality of Power (ICHQP)*, *IEEE Proceedings*, Belo Horizonte, 2016.

1 Introduction

This section covers the motives for creating this thesis and the scope of research, including the topics examined, but also stating what won't be covered. The contents and sections of the thesis will be outlined and briefly explained in subsection 1.4.

1.1 Motivation

Grid codes require decentralized power plants to stay connected to the grid during grid disturbances. Only under certain conditions the power generation unit is allowed to disconnect from the grid. Requirements and operating limits regarding voltage, frequency, power factor and active and reactive power control are defined in grid codes. In terms of the LVRT capability, voltage-against-time-profiles are given, varying in voltage dip depth and length, type of fault (e.g. 3-phase or 2-phase fault) and sometimes in voltage recovery shape.

First Grid codes were introduced around 1997. They were a set of technical guidelines and operation specifications designed for large conventional power plants in transmission systems. In distribution systems they aided as guidelines in planning and development for distribution system operators. The implementation of distributed generation in lower voltage levels was assessed by performing individual studies before integrating them, but there haven't been any specific grid codes around yet. Over the years, more and more renewables and distributed generation were introduced in low and medium voltage level networks. Therefore, what previously have been networks with passive components and loads mostly, became networks including a significant number of active components. This bidirectional power flow gave reason to re-design grid codes to consider power system levels below transmission system levels as well. [2, 3]

Prior to that, most grid codes did not require decentralized power plants to support the power system during grid disturbances. They were allowed to disconnect from the grid when an abnormal grid voltage was detected. With the increased penetration of distributed generation based on regenerative energy resources, disconnection of those power plants during grid disturbances would lead to a sudden loss of a decent amount of generation and therefore could generate problems regarding frequency and voltage in the system, leading as a worst case to a system collapse. As a consequence, low-voltage-ride-through-(LVRT)-requirements were determined. They specify voltage limiting curves, within which the power plant isn't allowed to disconnect from the grid. Figure 1.1 shows a selection of

LVRT-profiles of several countries' grid codes. The area defined by the ENTSO-E for type D[2] generators is also highlighted [4].

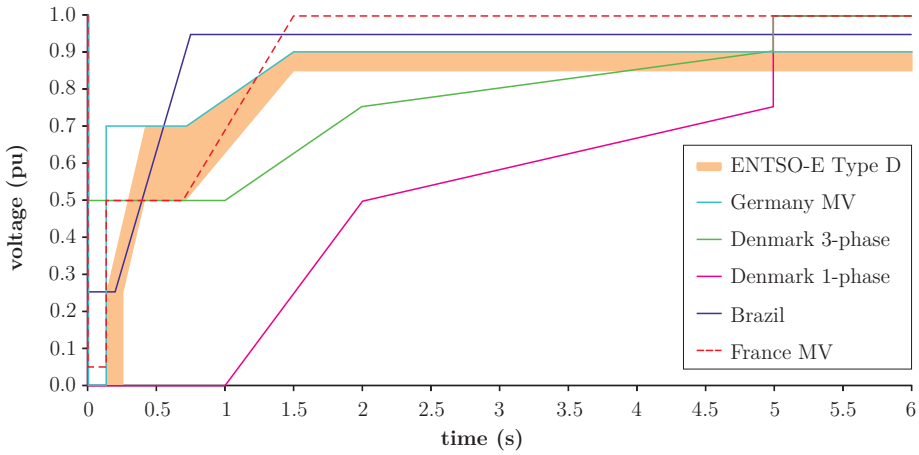

Figure 1.1: Comparison of LVRT limiting curves from grid codes of several countries

Grid codes differ from country to country due to different regulations and laws. The large variety of different grid codes makes it difficult for manufacturers to guarantee that their power generation units are able to fulfill different grid code requirements, if they are planned to be rolled out on an international level. Aside from that, some grid codes' requirements might be too stringent for some generation units to be able to comply with. Even if the same requirements as in another grid code are issued, but utilized in a different grid structure – e.g. weaker grid, in terms of short circuit power – they might not be practicable in that grid. Often times it's not clear on what base requirements in grid codes have been defined. The designing process is quite nontransparent in most grid codes. Besides, the requirements can be confusing and leave room for interpretation, which is contradictory to the idea of guidelines or standards. The number of different grid codes with different requirements and interpretations is not helping in this regard. However, in recent years a lot of work has been put into the harmonization of grid codes on an international level.

Especially voltage-against-time profiles given in grid codes' LVRT requirements sometimes include fault incidents to be withstood by power generation units, which are highly unlikely to occur in the grid. In order not to deny the connection of power generation units, which might be fine riding through almost all kinds of faults occurring in a certain grid, probabilistic considerations should also be regarded when designing LVRT requirements, which is not the case in most grid codes. In addition to that, the location (voltage level) of

[2] Power generation units with rated power output at 75 MW or above and connection point at 110 kV or above.

a fault event causing a severe voltage dip should be taken into account as well, because it can have an influence on how the voltage dip propagates through the grid and how many power generation units are affected. For example, denying the connection of a power generation unit to the low voltage network, because it's not able to ride through a severe fault – e.g. voltage dip down to a remaining voltage of u<0.05 pu – might not be reasonable, because if such a fault occurs, it's usually nearby (LV network busbar or a close MV network busbar) – otherwise the remaining voltage would be higher – and therefore, only a small amount of power generation would be affected and normally not compromising system security.

1.2 Scope of Research

The aim of this doctoral thesis is to deal with characteristics and factors influencing the LVRT capability of synchronous machines. This starts by examining requirements defined in grid codes and investigating how such requirements regarding LVRT capability of power generation units are established. The focus is on grid codes' LVRT requirements, i.e. the ability of a synchronous machine to ride through a fault, especially on voltage-against-time profiles. Another important topic regarding those requirements is how they should be interpreted, as this seems to be an often discussed issue. Other requirements specified in grid codes, such as frequency response, power factor specifications and active and reactive power control for example, are not regarded in detail. The issue of synchronous machines facing voltage rises and as a result disconnecting from the power grid due to protection device tripping won't be covered either. This matter is dealt with in so-called high-voltage-ride-through-(HVRT)-requirements. It is not intended to give an overview of currently existing grid codes. This doesn't seem to be practical, because of the huge number of different grid codes out there and the fact, that they are constantly updated. When needed, the guidelines drafted by entities of ENTSO-E [4] are used as reference for LVRT requirements.

The reasonability of voltage-against-time profiles in LVRT requirements should also be investigated. For this purpose fault statistics will be analyzed to determine the type of faults, remaining voltage and time duration of a fault and voltage levels affected. These results will be compared to typical LVRT requirements. In addition to that, investigations of how fault incidents propagate through a power grid will be performed based on simulations on a Central European power grid using real life data. Statements will be made, whether typical LVRT requirements are too harsh or justifiable.

Different test methods for establishing the LVRT capability of power generation units are discussed. The most common test method utilizing a shunt impedance based LVRT test container is investigated in more detail. In addition to that, the certification process based on tests using an LVRT test container will be examined in detail. Also, the influence such

a test equipment might have on the dynamic performance of a synchronous generator is analyzed.

All investigations performed are concerning 3-phase short circuits only, because as real life tests and literature research have shown, 1-phase and 2-phase faults are rarely problematic in terms of the LVRT capability of a power generation unit. 3-phase short circuits are the most demanding faults in this regard.

1.3 Research Questions

The following research questions will be addressed in this thesis:

1. LVRT Profiles: Are the requirements regarding the LVRT behavior defined in current grid codes justified or too strict?
2. LVRT Testing: Are the state-of-the-art LVRT capability testing procedures reasonable?
3. Validation of LVRT capability: What are the significant parameters, methods and limitations of an LVRT validation procedure?
4. Improving LVRT capability: How can the LVRT capability of a synchronous machine be improved? What needs to be taken into account when dimensioning a series braking resistor?

1.4 Outline of the Thesis

The remaining sections of this thesis are briefly outlined in the following.

- **Section 2: Literature Survey**
  Introductory topics relevant to this doctoral thesis' field of research are presented in this section. Characteristics and development of LVRT profiles are discussed and light is shed on the often times confusing matter of how to interpret them. A brief overview about dynamic models relevant for power system analysis is given. Concluding this section, basic simulation methods are introduced.

- **Section 3: Likelihood of Severe Voltage Dips**
  In this section voltage sags due to short circuits in transmission and distribution grids are investigated. Introductory, statistics of fault events and voltage dips are presented, to give an idea about the probability of certain faults and voltage dips. The severity and propagation of such faults is assessed through simulations performed on a detailed Central European power grid. Results show how faults propagate through different

voltage levels in a grid structures as given here and how confined areas of severely low voltages due to a fault event actually are.

- **Section 4: LVRT Testing**
  This section deals with LVRT testing. First, an overview about different LVRT capability test methods is provided. Afterwards, an equipment testing standard for wind turbines is introduced.
  Finally, the validation procedure of LVRT simulation models of decentralized power plants is discussed. The certification and validation procedure is presented as it is customary in Germany. The certification of power generation units through validation of simulation models is discussed in more detail. Experiences gathered in a case study, where gas-engine driven power generation units needed to be validated, are presented. Results of this validation process are shown as well.

- **Section 5: Limitations of LVRT Testing**
  The influence of a variation in short circuit power at the point of common coupling on the dynamic behavior of a synchronous generator is examined, since this is an often times neglected factor, when assessing the LVRT capability of generation units. As outlined in section 4, there are several different methods to test power generation units for their LVRT-capability. The influence of the most common LVRT test equipment – a shunt impedance based test container – on the dynamic performance of a power generation unit is studied in this section. Findings based on the results of a case study performed in a power systems analysis software are discussed and recommendations for enhancing the test procedure are given.

- **Section 6: LVRT Capability Improvement**
  Methods aiding to improve the LVRT capability of a power generation unit are briefly outlined at the beginning of this section. The theory behind the so-called backswing phenomenon is elaborated, which describes the behavior of synchronous machines in the first few milliseconds of a fault event. A series braking resistor is introduced as a retardation device for decentralized power plants. This device mitigates the acceleration of a synchronous machine's rotor during a fault event, to prevent the machine from losing synchronism with the power grid. The series resistor design and the control strategy are presented. A case study performed in a power systems simulation software shows the performance of such a retardation device based on a real life setup.

- **Section 7: Conclusion and Outlook**
  This section concludes the thesis as regards content, by summarizing the findings of all topics and issues discussed. Furthermore, the research questions will be answered and an outlook for possible future work is given.

2 Literature Survey

This section covers literature and topics most relevant for this thesis. Findings from this survey are the basis for further in-depth analyses. Insight into the development procedure of LVRT profiles and how they are to be interpreted is given. Basic simulation models and simulation methods are briefly introduced as well.

2.1 LVRT Profiles

Due to the large number of different grid codes and LVRT requirements available worldwide there are oftentimes discussions and confusions on how to interpret certain requirements. Especially the voltage-against-time profiles given in LVRT requirements can be somehow misleading and are therefore misinterpreted quite often. Amongst other things this can be attributed to the fact that depending on the grid code, the voltage-against-time profiles are to be interpreted differently. Besides, grid code guidelines can be unclear and not directly state how certain LVRT requirements have to be interpreted. Sometimes only additional documents (if available) shed light on the subject. This subsection gives a few examples of common grid codes and how they are to be understood. This should help to get a grasp on how to interpret most voltage-against-time profiles.

The most critical and most debated parameters are the remaining voltage and the fault clearing time, because they can have a significant impact on the design of generators and their control strategy. The fault clearing time is critical for rotor angle stability of synchronous generators, because the rotor accelerates during the fault due to the lack of dissipated power. Longer fault durations require more rotational masses in order to increase the generator's inertia and with it limit the rotor acceleration[3]. However, the stability is not only affected by the fault clearing time, but also by the generator's pre-fault operating point. [5]

2.1.1 Shape of LVRT Profiles

In general, voltage-against-time profiles can be classified into two groups:

- Rectangular voltage dips
- Polygonal voltage dips

[3] Regarding this issue see also section 6 "LVRT Capability Improvement".

Polygonal profiles with recovery ramp can be obtained by statistical analysis of network failures.

In Figure 2.1 the ENTSO-E FRT profile of a power-generating module is shown. The voltage and time setpoints depend on the voltage level the generator is connected to and the capacity of the generator. Each point on the profile represents a voltage level and a corresponding fault duration, which the EUT has to ride through in order to pass LVRT requirements specified by this profile. Specific values or ranges for the given timestamps and voltage setpoints can be found in [4]. It is not a voltage-against-time curve obtained by plotting the transient voltage response due to a disturbance. The line marks the lower voltage boundary, rather than any characteristic voltage behavior. [6]

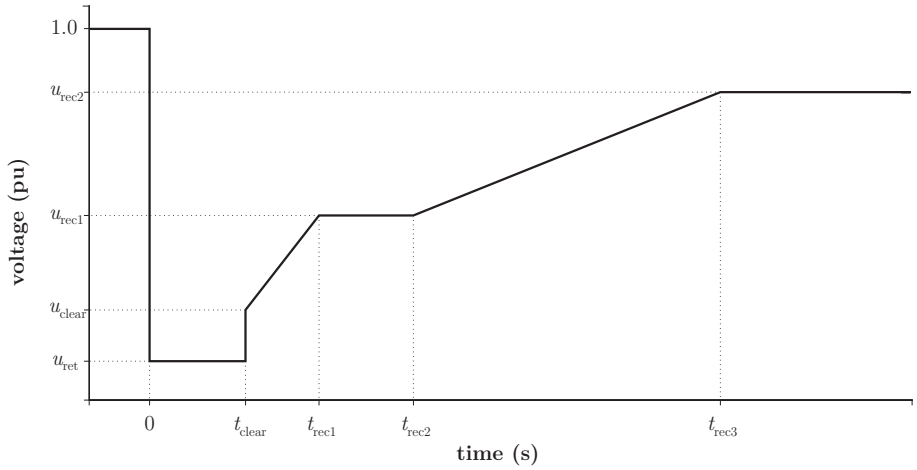

Figure 2.1: ENTSO-E fault-ride-through profile of a power-generating module [4]

Figure 2.2 illustrates examples of several individual fault events of rectangular shape incorporated in the ENTSO-E FRT profile.

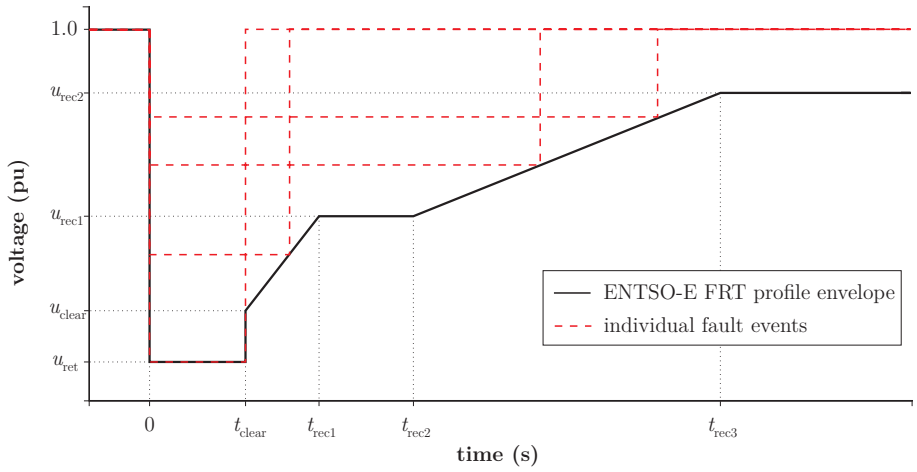

Figure 2.2: Random individual fault events within the ENTSO-E FRT profile

According to an ENTSO-E document from a meeting of a DSO technical expert group the voltage profile given in ENTSO-E standards is to be understood as an envelope of voltage dip curves, rather than an exact voltage curve, that has to be withstood by the EUT. [7] The "Implementation Guideline for Network Code Requirements for Grid Connection Applicable to all Generators" [5] also states that the FRT guidelines do not require the actual voltage recovery curve of the EUT to be the shape of the voltage-against-time profile given by ENTSO-E, but rather represent a lower limit of it, which means the curve can be seen as data pairs of different voltage dip depth and length. So the FRT profile defines boundaries of voltage-against-time-curves, i.e. regions where the generator is allowed to trip or not to trip. It represents the boundaries of a voltage-against-time profile, showing at which individual voltage drop and fault clearing time the synchronous generating unit must stay connected to the grid. The curve itself is not a voltage dip curve, because the voltage recovery depends among other things on the generator data (time constants, reactances, and inertia), system configuration, load flow and voltage dependency of loads. [8, 9] The document "Frequently Asked Questions" [10] given by the ENTSO-E also clarifies that the actual voltage recovery curve does not have to be the shape of the voltage-against-time profile. The actual voltage recovery curve has a freely controlled response during the post-fault period, which strongly depends on the EUT technology and the short circuit power at the grid connection point.

Bollen [11] explains slow the post-fault voltage recovery by the starting of induction machines. Due to the voltage sag during the fault the induction motors will slow down. The torque of an induction motor is proportional to the voltage squared, so even a small voltage dip can lead to a considerable drop in torque and with it in speed. When the fault event is cleared and the voltage comes back, the induction machines attempt to re-accelerate, resulting in drawing an excessive amount of current – up to ten times their nominal current – from the power supply. So immediately after the fault, induction machines behave similar to short-circuited transformers. This prevents fast voltage recovery and thus influences the shape of voltage sags. These post-fault inrush currents of induction machines can lead to extended voltage sags and last several seconds. This effect is more pronounced as the number of induction machines or the fault duration increases. [12, 13]

The "Wind Generator Task Force" [14] provided a white paper for the development of a new VRT standard. One of their working packages was to define a boundary for the voltage recovery excursion that occurs between the time a transmission fault is cleared and the time the transmission voltage returns to u=0.9 pu, which is the lower boundary of continuous operation. The shape of the voltage recovery boundary was determined by investigating a representative sample of Zone 2[4] three-phase faults with normal fault

[4] Fault located by distance relay over 75 % of the distance from the relay to the end of the line.

clearing (time period of approximately 4-9 cycles) provided by local TSOs. Figure 2.3 shows fault event data plotted as points, marking the voltage dip depth and the duration of the fault, and the fitted VRT recovery boundary curve.

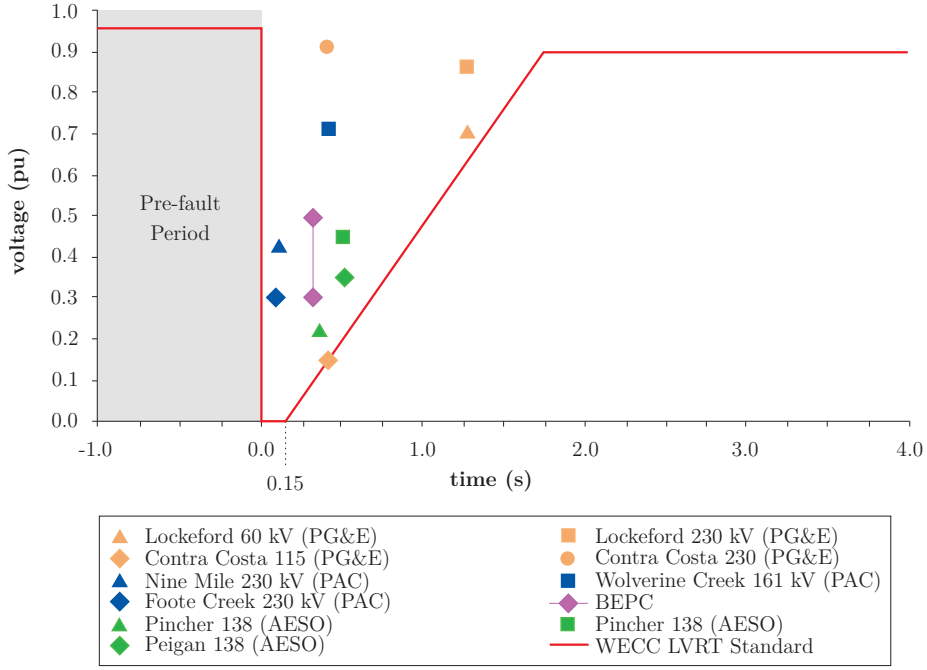

Figure 2.3: LVRT profile fitted to actual fault events data [14]

This means that their voltage-against-time profile also represents a lower voltage boundary, rather than an actual transient voltage curve that could be obtained by plotting the transient voltage response at a point in the system (e.g. the PCC) against time. The profile doesn't necessarily represent the actual shape of voltage dip curves of any of the recorded fault events.

Qureshi and Nair [15, 16] present the development of a voltage envelope for LVRT requirements for the New Zealand transmission system. In order to acquire a single voltage envelope for the whole network or a particular transmission level a limited set of worst voltage responses of network buses due to fault events were selected. They are suggesting to either average them out or to select the most critical voltage response in terms of remaining voltage and fault clearing time. They also recommend considering all possible contingencies to determine one single voltage duration profile.

The distinction between specific voltage profiles associated with real events and the concept of applying a voltage profile based on a locus of fault events data is very important. The interpretation and definition of how the voltage is recovering from a fault event can have a large impact on the transient behavior and with it the stability of a generator. Especially

if a slowly rising voltage recovery ramp is utilized, which is highly demanding in terms of rotor angle stability.

Another issue besides causing confusion when utilizing the concept of a voltage envelope as a FRT profile instead of several individual rectangular ones is that the envelope represents an infinite number of individual fault events. So if one wants to test a generating module against the ENTSO-E FRT profile for example, compromises have to be made.

The lower voltage level after the recovery period of usually around u=0.9 pu is explained due to a possible weaker grid configuration after the disconnection of the faulty network component, which caused the fault. Another possible scenario is the case of a self-extinguishing fault, where the system will return to its pre-fault conditions. [17, 18]

Östman et al. [19] conclude from their simulation results that the most critical factors performing LVRT tests have not been fault clearing time and voltage dip depth only, but more so when a slow voltage recovery curve was employed in simulations. According to their findings, it was not possible to remain synchronism utilizing a recovery slope. They also mention that when a fault is cleared, their simulations show that the voltage recovers almost immediately. Induction motors and transformers will take an inrush current to re-accelerate and to magnetize that may give a tail in the voltage dip, but the shape would still be mainly rectangular.

2.1.2 Fault Clearing Time

The fault clearing times for the most severe voltage dips in terms of remaining voltage given in LVRT requirements are determined relay, breaker and telecommunication performance given in the specific region where the grid code applies [9]. In Continental Europe faults are usually cleared within 100-150 ms [6, 20]. Due to a fault event in 2003 in Sweden, where a fault was not cleared within that time due to further failure of equipment, a black-out covering southern Sweden and part of Denmark including Copenhagen was the result. Based on this experience a political decision was made to invest in further resilience of the network to withstand even such a double contingency. Therefore, the ENTSO-E network code requires generators to ride through severe faults up to clearing times of 250 ms. [20]

The ENTSO-E implementation guideline notes that a fault clearing time of around 150 ms could be requested regardless of the generator's operating point, whereas fault durations in the range of 250 ms could only be applied for a limited area of pre-fault operating points. Therefore, it would be insufficient to specify fault clearing times without specifying generator operating conditions under which successful FRT performance is required. [5]

Abbey and Joos [21] perform system studies to demonstrate its benefits while establishing a relationship between the shape of the characteristic and the strength of the

interconnection. They state that the fault clearing time is dictated by the length of time it normally takes to clear a transmission level fault (10-20 cycles), which is dictated by protection technologies and the location and type of fault. According to their studies the slope of the recovery voltage ramp likely depends on the strength of the interconnection and reactive power support.

2.1.3 Fault Location

Another issue is the definition of the fault location. Mostly it's defined at the PCC, rarely at generator terminals. Both fault locations come with inherent problems. Depending on the EUT, testing the LVRT capability with the fault position at generator terminals might not be possible on some sites. The problem with testing at the PCC is that the performance of the generator heavily depends on the lines and transformer(s) in between the generator and the PCC. Given a certain LVRT profile, not only the pre-fault operating point of the generator is crucial to the capability of riding through the fault event without disconnecting from the grid, but also the SCR at the fault location. The SCR is the ratio between the short circuit power at the fault location and the nominal power of the EUT. The higher the SCR, the stronger is the grid considered. Nonetheless, very rarely are requirements regarding the SCR given in grid codes. [9]

The remaining voltage for shorter fault durations is set to zero in a lot of grid codes. For a fault location on transmission level the remaining voltage will be zero for the phases affected by the fault, but it is unrealistic, that a zero retained voltage sustains on a distribution level for transmission system faults, because the transformers between transmission system and lover voltage levels will limit the voltage drop seen at those lower levels in case of a transmission system fault. [5]

2.2 Dynamic Models

To achieve satisfying results in dynamic transient system analysis, simply modeling synchronous machines by a simple voltage source behind an impedance isn't sufficient. Fortunately there are well established higher order models available in literature and very well integrated in most power system analysis tools. The specific models are not discussed in detail here. For further details see the relevant references.

Kundur [22] provides a detailed insight into the theory and modeling of synchronous machines and how they can be represented in stability studies. Models of higher order are given, depending on the assumed number of rotor circuits to be present. In addition to that, standard parameters, typical values and approximation guidelines are presented. Simplifications to reduce the order of the synchronous machine model are also mentioned,

which might be useful for simulations, where computation time is more critical than a very good representation of the dynamic behavior.

Furthermore, the IEEE standard 1110-1991 [23] focuses on the modeling of synchronous machines in stability studies. It categorizes three d-axis and four q-axis models, depending on the number of rotor circuits representing the machine. Assumptions made in each model are discussed. Investigations are divided into large-disturbance nonlinear analysis and small disturbance linear analysis. Different saturation algorithms and parameter determination guidelines are presented as well.

Since the share of inverter based generation is still increasing in most countries, it needs to be regarded in power system studies. The Electric Power Research Institute (EPRI) in collaboration with the Western Electricity Coordination Council (WECC) has developed models of wind turbine generators for power system simulations. The models given only regard the inverter, not the mechanical structure or the generator. [24]

2.3 LVRT Simulation

In many power system analysis programs there are basically two dynamic simulation methods available: the instantaneous value simulation (EMT – Electro-Magnetic Transients) and the transient stability simulation (RMS – Root Mean Square). RMS simulation models are equivalent to fundamental frequency models, where the stator flux electromagnetic transients are neglected in the model equations, whereas in EMT simulations they are not neglected. This simplification in RMS models comes with the big advantage of reduced simulation times.

Sørensen et al. [25] advocate RMS simulations when big, complex systems or long events need to be simulated, whereas EMT simulations are advised for example when considering fast protection equipment, which might trigger to current oscillations that are only represented in EMT simulations. For long-term system stability analysis – which is not affected by stator flux transients, if no fast relays are tripped – RMS simulations are sufficient.

Aside from the already mentioned advantages of RMS simulations, Ortojohann et al. [26] note that reducing the computational time also reduces the costs of simulation equipment, while achieving almost similar results compared to EMT simulations.

Simulations to validate the LVRT capability of synchronous machines are required to be performed by means of RMS simulations, as stated in technical guidelines by the "Federation of German Windpower and other Renewables – FGW" [27]. The reason being once again the reduced computation time of RMS models, especially when larger power generation sites need to be simulated and validated.

Nevertheless, for in-depth analyses of transient events, such as the backswing phenomenon (see subsection 6.2), EMT simulations are essential to capture such events properly.

2.4 Conclusion

In this section some basic literature relevant for this thesis has been mentioned. Light has been shed on the often times discussed and confusing topic of how to interpret LVRT profiles in grid codes. Especially the voltage recovery profile can be misleading. It was clarified, that each point on the voltage-against-time-characteristic represents a combination of voltage and associated time duration, which the connected generator must ride through, instead of an actual transient voltage curve. Real life examples on how LVRT profiles are established in certain cases have been shown also. Other factors impacting the LVRT behavior of a power generating unit were also discussed, such as the fault clearing time and the location of the fault event. It can be concluded that designing LVRT profiles for absolute extremes or unlikely operation conditions is neither economical nor desirable in the long run as desired features.

In addition to that, basic simulation models for dynamic power system analysis have been introduced. Since they are very well established and standard models for this kind of studies, they weren't discussed in detail, but only referenced to key literature. Since inverter based generation has been drastically increasing in the past, simulation models for this type of generation was also covered.

Finally, RMS and EMT simulation methods have been outlined, including their advantages and disadvantages. Both methods are investigated in more detail in subsection 6.2.2.

3 Likelihood of Severe Voltage Dips

The capability of power generation units to withstand a defined voltage-against-time-profile is specified by LVRT requirements. Typical are LVRT profiles with remaining voltages around u=0.05 pu for a fault event duration in the range of 150-250 ms. Statistics of fault events from different regions and countries worldwide are presented to provide a rough estimate about the of certain fault events in specific countries or regions. Complementary to that, the propagation of voltage sags through different voltage levels in a Central European power grid and the likelihood of such low voltages, as given by voltage-against-time-curves in grid codes, is investigated. It is not intended to make statements about the LVRT-capability of power generation units. Simulations are performed on an actual power grid with real load flow data with the power systems analysis software DIgSILENT PowerFactory.

3.1 Introduction

The driver in development of LVRT requirements was the speculation that voltage sags – caused by faults – might lead to area-wide tripping of generation and thus causing a severe threat to frequency stability. Regarding the possible wide-area tripping of generation, basically two scenarios have to be considered:

- Fault on the transmission level:

  Faults on the transmission level are rare compared with faults in distribution systems, but a large area will experience a voltage sag. Depending on synchronous generation installed, the region of remaining voltage below u=0.2 pu will be limited. Underlying sub-transmission and distribution systems will be affected by the sag at the connection point to the transmission system.

- Fault on a sub-transmission level:

  In the worst case, the complete concerned sub-transmission grid will be affected by a severe dip during the fault. However, the total amount of possibly tripping generation is rather limited and not significant for frequency stability.

To confirm the statements, a real power grid in Central Europe is analyzed. Voltage sag propagation analyses are performed on different voltage levels by means of simple short circuit calculations.

Voltage sags are mainly caused by faults in the system. Starting of large loads can also lead to voltage sags, but they are usually not as severe in terms of voltage dip depth, although they can last longer than typical short circuits (in the range of seconds to tens of

seconds). The focus of this section's study is on three phase short circuits, because they are the most severe ones regarding LVRT. One has to keep in mind, that such types of faults occur very rarely compared to 2-phase and phase-to-ground faults, which is shown in subsection 3.3 "Fault Statistics". [11]

For a simple grid structure as shown in Figure 3.1, the remaining voltage at a certain substation can be easily determined by hand with equation (3.1). As an approximation it is eligible to neglect the load current, since the short circuit current is usually much higher. The red flash indicates the fault location, E is the inner voltage of the source, Z_S the source impedance, Z_F the impedance between the fault location and the PCC and U_{ret} is the remaining voltage at the PCC.

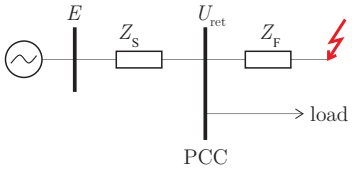

Figure 3.1: Exemplary grid structure

$$U_{ret} = E \cdot \frac{Z_F}{Z_S + Z_F} \tag{3.1}$$

The short circuit power levels S_{PCC} at the PCC and S_{Fault} at the fault location can be calculated as follows:

$$\begin{aligned} S_{PCC} &= \frac{U_n^2}{Z_S} \\ S_{Fault} &= \frac{U_n^2}{Z_S + Z_F} \end{aligned} \tag{3.2}$$

Combining equations (3.1) and (3.2) the remaining voltage U_{ret} can be expressed by means of short circuit power levels, as shown in equation (3.3).

$$U_{ret} = E \cdot \frac{Z_F}{Z_S + Z_F} = E \cdot \frac{Z_F + Z_S - Z_S}{Z_S + Z_F} = E \cdot \left(1 - \frac{Z_S}{Z_S + Z_F}\right) = E \cdot \left(1 - \frac{\frac{U_n^2}{S_{PCC}}}{\frac{U_n^2}{S_{Fault}}}\right) = E \cdot \left(1 - \frac{S_{Fault}}{S_{PCC}}\right) \tag{3.3}$$

Typical short circuit power levels in a Central European power grid – which is introduced in more detail in subsection 3.5.1 – are as follows:

- 380 kV: 14 VGA
- 220 kV: 7 GVA
- 110 kV: 2 GVA

Of course the actual short circuit power level of each individual substation can vary, depending on its location. For example it's higher than given above, if it's located near an area of concentrated generation and vice versa.

With equation (3.3) and the short circuit power levels given above, the remaining voltages can be approximated for a radial feeder, depending on the fault location (see Table 3.1). This approximation yields satisfying results, as was confirmed by simulations, but only for radial feeders as illustrated in Figure 3.2, where the voltage source (power generation) is located at one end of the feeder.

Table 3.1: Approximated remaining voltages depending on fault location

Fault location	**Remaining voltage at**		
	380 kV	220 kV	110 kV
380 kV	0 %	0 %	0 %
220 kV	50 %	0 %	0 %
110 kV	86 %	71 %	0 %

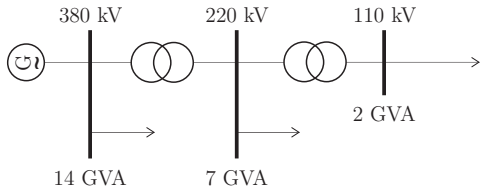

Figure 3.2: Exemplary radial feeder structure

This simple approximation of remaining voltages due to short circuits on different voltage levels provides a rough first assessment of the propagation of voltage sags throughout a grid. In a meshed grid with spread generation among all voltage levels, the calculation of remaining voltages is more complex and therefore performed by means of computer simulations. The following subsections are going to discuss the simulation of voltage sag propagation based on simulations performed on a Central European power grid. The remaining voltages in the power grid during a fault event are determined with sufficient accuracy by means of short circuit calculation. Dynamic simulations could be performed to calculate how the voltage develops over time in detail during the fault event. However, for this type of simulation the models of generators, controllers, governors and data of grid components in general have to be quite accurate to get satisfying results. Besides, dynamic simulations of large grids can be computational intensive and time consuming. Therefore – and since they prove to be accurate enough – short circuit simulations are chosen to be an adequate tool for this type of investigation.

3.2 Short Circuit Calculation Methods

The most common method for AC short circuit calculations is given by the IEC 60909 standard. This method is suitable for calculations performed at the planning stage, where the system operation conditions are not yet known, and therefore assumptions have to be made. They are usually carried out to dimension equipment properly and to aid the design of the protection scheme. The method uses an equivalent voltage source at the short circuit location and works independently of the load flow (operating point) of the system. Correction factors for voltages (c-factor) and impedances are used to give conservative results. All line capacitances, shunt admittances and non-rotating loads, except the ones of the zero-sequence system, are neglected.

The complete method, also known as superposition method, is based on the same approach, but takes the pre-fault operation state of the system into account as well, and therefore is a more accurate method. The superposition method calculates the expected short circuit currents based on the existing network operation conditions. It considers the excitation conditions of the generators, the tap changer positions of the transformers and switching settings also. From this pre-fault condition the pre-fault voltage of the faulted busbar can be calculated. For the pure fault condition the negative pre-fault busbar voltage is connected at the fault location and all other sources are set to zero. Since network impedances are assumed to be linear, the system condition after the fault event can be determined by superimposing both the pre-fault and pure fault conditions [28], [29].

3.3 Fault Statistics

Following, fault statistics for different countries and regions are given to provide a rough estimate about the probability of different types of faults, fault locations and fault events in general.

3.3.1 Austrian Transmission Grid

According to the Austrian transmission grid operator, fault statistics over the last 10 years show that around 4-5 fault incidents occurred per 100 km of line length on the 380 kV and 220 kV transmission levels combined per year. This includes 1-phase, 2-phase and 3-phase faults. Automatic reclosing is also considered in this statistic. Fault incidents of substations are also given with around 2.4 events per year.

To get an idea of the ratio between 1-phase, 2-phase and 3-phase faults, fault statistics of a 220 kV double-circuit line are given in Table 3.2. Both circuits span roughly 100 km of line length. The observation period is almost 7.5 years. Fault events are divided into 1-

phase, 2-phase and 3-phase faults, including automatic reclosing. The statistic also notes if both circuits were affected by the fault event.

Table 3.2: Fault Statistics of a 220 kV Double-Circuit Line

Circuit	**1-phase**	**2-phase**	**3-phase**	**Sum**
1	61.9 %	2.4 %	2.4 %	66.7 %
2	14.3 %	2.4 %	16.7 %	33.3 %
1 & 2	76.2 %	4.8 %	19.0 %	100.0 %

As the fault statistic indicates, the majority of faults are 1-phase faults. Only 19 % of all faults were 3-phase faults. It has to be noted that the faults in Table 3.2 are not necessarily bolted. The fault impedance depends on the fault origin, which is lightning in most cases. There are more 3-phase than 2-phase faults, because a lot of 2-phase faults tend to evolve into 3-phase faults given the fault origin.

3.3.2 France

A statistic of fault events in the French transmission and sub-transmission systems presents the number of faults per year and 100 km. They are categorized into single-phase and poly-phase faults and depending on the voltage level. Table 3.3 summarizes the results of the statistic. [30, 31]

Table 3.3: Fault statistics of French transmission and sub-transmission lines [31]

Voltage Level	**Single-phase**	**Poly-phase**	**Event Total**
63 kV	17.3	6	23.3
90 kV	11	3.3	14.3
225 kV	9.9	2.2	12.1
400 kV	3.3	0.5	3.8
Event Total	41.5	12	53.5

The data shows that less than 23 % of all fault events were 2-phase or 3-phase faults. Furthermore, mostly medium voltage levels seem to be affected, whereas only 7 % of all events have been detected on the 400 kV voltage level.

3.3.3 Nordic and Baltic Countries

The Nordic countries Denmark, Finland, Iceland, Norway and Sweden were part of the Nordel association for electricity co-operation. On 1. July 2009 Nordel was wound up and

all operational tasks were transferred to ENTSO-E. The ENTSO-E is publishing annual reports about grid disturbance statistics. The report by ENTSO-E [32] gives an overview of the Nordic and Baltic HVAC transmission grid disturbance statistics. The following tables include data covering faults causing disturbances in the 100-420 kV grids of Denmark, Finland, Iceland, Norway, Sweden, Estonia, Latvia and Lithuania. In Table 3.4 fault statistics for overhead lines are shown for the time period 1996-2014. Cable faults statistics are shown in Table 3.5 for the period 2005-2014. More detailed information for each Nordic and Baltic country is shown in ENTSO-E [32].

Table 3.4: Overhead line faults and cause allocation in Nordic and Baltic countries between 1996-2014 (total number shown) [32]

Voltage Level	**Number of faults**	**Faults divided by cause (%) during the period 1996–2014**								
	1996-2014	Light-ning	Other environ-mental causes	External influence	Opera-tion and main-tenance	Tech-nical equip-ment	Other	Unknown	1-phase faults	Perma-nent faults
380-420 kV[5]	88	43.1	36.2	1.6	2.5	2.6	1.9	12.1	72.6	7.0
220-330 kV	111	47.5	23.8	5.7	1.2	4.7	3.3	13.8	65.7	8.1
100-150 kV	737	48.2	16.8	3.0	1.9	2.4	3.0	24.9	50.6	6.4

Table 3.5: Cable faults and cause allocation in Nordic and Baltic countries between 2005-2014 (total number shown) [32]

Voltage Level	**Number of faults**	**Faults divided by cause (%) during the period 2005–2014**						
	2005-2014	Light-ning	Other environ-mental causes	External influence	Operation and mainte-nance	Technical equipment	Other	Unknown
380-420 kV[5]	0.8	0.0	0.0	0.0	0.0	66.7	16.7	16.7
220-330 kV	2.1	5.9	0.0	0.0	11.8	70.6	0.0	11.8
100-150 kV	10.4	0.0	2.9	10.1	7.2	58.0	7.2	14.5

It can be seen that the main reason for overhead line faults are lightning and other environmental causes and the majority of faults are 1-phase faults. The main reason for cable faults is due to technical equipment failure.

The shares of different fault types for Finland's transmission system are presented in Table 3.6. It can be seen that the vast majority of faults (around 80 %) are 1-phase earth faults at every transmission voltage level. 3-phase short circuits with around 3 % are very rare.

[5] Nordic countries only.

Table 3.6: Fault frequencies and shares of fault types for Finnish transmission systems [33]

Voltage	**Fault frequency**	**Shares of different fault types**			
kV	Faults per year per 100 km	1-phase earth faults	2-phase short circuits	3-phase short circuits	2- or 3-phase earth faults
400	0.28	80 %	2 %	3 %	15 %
220	0.72	78 %	2 %	3 %	17 %
110	3.5	81 %	3 %	2 %	14 %

3.4 Voltage Dip Statistics

To give a better idea about the effect of fault incidents, voltage dip statistics about remaining voltages and fault durations of certain countries are given in this subsection.

3.4.1 United States and Canada

A comprehensive investigation regarding power quality was conducted in the US and Canada by the National Power Laboratory (NPL), the Canadian Electrical Association (CEA) and the Electric Power Research Institute (EPRI). Since only EPRI was investigating medium voltage networks, only their results will be shown. Between 1993 and 1995 medium voltage networks ranging from 4.16 kV to 34.5 kV and line lengths from 1-80 km were monitored. The data is split into feeder and substation events. The events are categorized in fault event duration and voltage magnitude. Results for events per year are shown in Table 3.7 and Table 3.8. [30, 34]

Table 3.7: Substation events per year [34]

Remaining voltage	**0-100 ms**	**100-167 ms**	**167-333 ms**	**333-500 ms**	**0.5-1 s**	**1-2 s**	**2-10 s**	**10 s-8 h**	**Event Total**
80-90 %	28.3	6.1	3.0	1.3	1.9	0.6	0.4	0.1	41.7
70-80 %	8.1	2.6	1.2	0.4	0.4	0.1	0.2	0.0	13.1
50-70 %	5.0	1.5	1.0	0.2	0.3	0.1	0.1	0.0	8.3
10-50 %	1.1	0.4	0.4	0.1	0.1	0.0	0.4	0.0	2.5
0-10 %	0.2	0.1	0.4	0.8	0.5	0.9	1.1	1.4	5.4
Event Total	42.7	10.7	6.0	2.8	3.2	1.8	2.3	1.5	71.0

Table 3.8: Feeder events per year [34]

Remaining voltage	**0-100 ms**	**100-167 ms**	**167-333 ms**	**333-500 ms**	**0.5-1 s**	**1-2 s**	**2-10 s**	**10 s-8 h**	**Event Total**
80-90 %	27.6	6.5	3.1	1.4	1.8	0.5	0.4	0.1	41.4
70-80 %	8.1	2.2	1.1	0.3	0.5	0.1	0.1	0.0	12.5
50-70 %	5.7	1.7	1.1	0.2	0.3	0.1	0.2	0.0	9.4
10-50 %	3.5	1.0	0.7	0.3	0.2	0.2	0.6	0.0	6.5
0-10 %	1.6	0.1	0.2	0.6	0.5	1.1	2.3	1.7	8.1
Event Total	46.5	11.5	6.2	2.8	3.3	2.1	3.7	1.9	77.9

This data shows that for both substations and feeders 75 % of all fault events are cleared within 167 ms. Looking only at those events, merely 3 % of substation events and 10 % of feeder events resulted in remaining voltages below 0.5 pu.

3.4.2 France

The Council of European Energy Regulators provides a benchmarking report on the quality of electricity supply, which includes several countries' fault statistics. The average number of voltage dips per year in the transmission network for France is shown in Table 3.9.

Table 3.9: Average number of voltage dips in transmission networks in France in 2009 [35]

Remaining Voltage u in [%]	**Duration in ms**			
	$10 \leq t \leq 200$	$200 < t \leq 500$	$500 < t \leq 1.000$	$1.000 < t \leq 5.000$
$90 > u \geq 80$	32.00	2.30	0.86	0.78
$80 > u \geq 70$	7.10	0.54	0.40	0.08
$70 > u \geq 40$	4.60	0.45	0.33	0.10
$40 > u \geq 5$	0.77	0.25	0.11	0.01

According to this table 89 % of all faults are cleared within 200 ms and 72 % have remaining voltages higher than u=0.8 pu.

3.4.3 Brazilian Power Grid

A power quality monitoring system was installed at over 250 locations in a distribution system in the south-east of Brazil. Harmonics, short-duration voltage variations, voltage imbalances, frequency deviations and other power quality disturbances were monitored for over more than two years. Measurements were conducted at voltage levels between 13.8-138 kV, although the data shown in the report doesn't give separate numbers for each voltage level. The number of events per voltage sag magnitude level is shown in Table 3.10. Table 3.11 shows the number of events with certain fault clearing times.

Table 3.10: Number of events with a certain voltage sag magnitude in Brazilian power grid [36]

Voltage sag magnitude	0-10 %	10-20 %	20-30 %	30-40 %	40-50 %	50-60 %	60-70 %	70-80 %	80-90 %
Number of events	0.1 %	0.5 %	0.7 %	1.5 %	3.7 %	4.6 %	8.1 %	20.2 %	60.6 %

Table 3.11: Number of events with a certain fault clearing time in Brazilian power grid [36]

Voltage sag duration	0-83 ms	83-167 ms	167-333 ms	333-833 ms	0.83-1.33 s	1.33-1.83 s	1.83-3 s	> 3 s
Number of events	59.3 %	20.4 %	6.7 %	9.5 %	2.8 %	0.7 %	0.3 %	0.3 %

As can be seen in Table 3.10, more than 80 % of all events have a remaining voltage higher than u=0.7 pu. Similar to the results shown in subsection 3.4.1, the majority of faults (79.7 %) is cleared within 167 ms, a typical time range for most protection equipment clearing a fault.

3.4.4 Hungary

The Council of European Energy Regulators provides a benchmarking report on the quality of electricity supply, which includes several countries' fault statistics. The average number of voltage dips per year on the MV level for Hungary is displayed in Table 3.12.

Table 3.12: Average number of voltage dips in MV networks in Hungary in 2009 [35]

Remaining Voltage u in [%]	**Duration in ms**			
	$10 \leq t \leq 200$	$200 < t \leq 500$	$500 < t \leq 1.000$	$1.000 < t \leq 5.000$
$90 > u \geq 80$	86.3	7.9	4.8	5.1
$80 > u \geq 70$	25.2	2.3	1.4	1.1
$70 > u \geq 40$	21.2	2.0	1.0	1.2
$40 > u \geq 5$	4.9	1.0	0.4	0.2

According to this table 83 % of all faults are cleared within 200 ms and 63 % have remaining voltages above u=0.8 pu

3.4.5 Spain

A joint working group report on the voltage dip immunity of equipment and installations by CIGRE [18] provides statistics of voltage dips from almost 1.200 monitored sites in Canada, Portugal, United Kingdom, South Africa, USA, Australia and Spain. A statistic

about the distribution of voltage dips according to their ration of remaining voltage for the data obtained from Spain is given in Table 3.13.

Table 3.13: Number of voltage dips with a certain remaining voltage [18]

Remaining voltage in pu	**Number of events**	**Share in %**
0.95-1.00	247430	77%
0.85-0.95	31579	10%
0.75-0.85	11248	3%
0.65-0.75	8191	3%
0.55-0.65	5973	2%
0.25-0.35	5331	2%
0.45-0.55	4294	1%
0.35-0.45	4173	1%
0.15-0.25	2855	1%
0.05-0.15	413	0%

This table indicates that 87 % of all voltage dips have a remaining voltage above u=0.85 pu. Furthermore it has to be noted that only 2 % of all registered fault events had remaining voltages below u=0.45 pu.

3.4.6 Italy

CEER [35] provides amongst others voltage dip data of Italian networks. The voltage dips per year at MV busbars of HV/MV substations are presented in Table 3.14. Although, only a 10 % sample of the Italian networks was investigated.

Table 3.14: Average number of voltage dips per year at MV busbars of HV/MV substations in Italy in 2010 [35]

Remaining Voltage	**Duration in ms**			
u in [%]	$10 \leq t \leq 200$	$200 < t \leq 500$	$500 < t \leq 1.000$	$1.000 < t \leq 5.000$
$90 > u \geq 80$	31.5	6.4	1.6	0.4
$80 > u \geq 70$	15.5	4.4	0.5	0.1
$70 > u \geq 40$	22.6	4.8	0.4	0.1
$40 > u \geq 5$	8.5	1.3	0.2	0.0

Similar to other fault statistics shown, the majority of faults (79 %) are cleared within 200 ms.

3.4.7 Portugal

Statistics for fault events of Portugal's transmission networks (60 kV and 150 kV) are presented in CEER [35]. The data has been obtained from measurements at 7 connection points.

Table 3.15: Average number of voltage dips per year in the transmission network in Portugal in 2009 [35]

Remaining Voltage	**Duration in ms**				
u in [%]	$10 \leq t \leq 100$	$100 < t \leq 250$	$250 < t \leq 500$	$500 < t \leq 1.000$	$1.000 < t \leq 3.000$
$90 > u \geq 80$	17.7	10.1	1.6	0.6	1.6
$80 > u \geq 70$	7.4	3.6	0.9	1.6	0.3
$70 > u \geq 60$	4.0	2.7	0.7	1.9	0.3
$60 > u \geq 50$	3.9	0.9	0.7	0.4	0.1
$50 > u \geq 40$	3.4	0.1	0	0	0.3
$40 > u \geq 30$	2.6	0.6	0.1	0.1	0.1
$30 > u \geq 20$	1.6	0.3	0.6	0	0
$20 > u \geq 10$	1.7	0	0.1	0	0
$10 > u \geq 1$	0.3	0	0	0.1	0

Almost 82 % of voltage dips are cleared within 250 ms. More than 57 % are cleared even within 100 ms.

3.5 Case Study

Following up on voltage dip statistics, simulations are performed to determine the voltage sag propagation in a power grid when facing 3-phase short circuits. The simulations are performed with the power systems analysis software DIgSILENT PowerFactory. The input for the simulations is a detailed model of a Central European power grid and all its neighboring countries.

3.5.1 Simulation Setup

The electrical power grid under study includes the most relevant elements of voltage levels between 10 kV and 380 kV. The 220 kV and 380 kV systems are represented in detail. Some loads and generators are aggregated in equivalent elements, representing the net load of a certain area or connection point, especially for voltage levels below 220 kV. Figure 3.3 gives an overview of the power grid and its basic voltage levels.

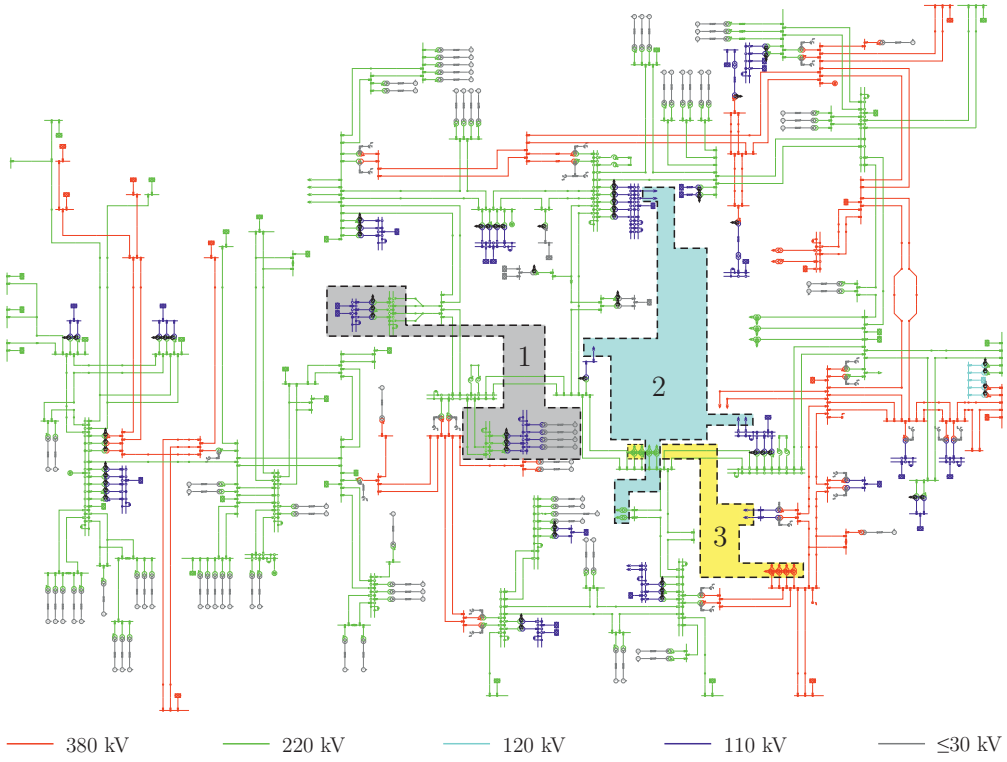

Figure 3.3: Overview of voltage levels in studied power grid and location of underlying 110 kV grids 1-3

Neighboring countries and lower voltage grid segments, such as densely meshed urban networks, are embedded in underlying grids and not explicitly shown in Figure 3.3. Three detailed 110 kV grids are implemented as underlying grids to investigate the impacts on sub-transmission levels. The connection points and locations of these grids within the studied power grid are highlighted in Figure 3.3. There are no direct interconnections between these grids. Henceforth, they will be addressed as 110 kV grids 1, 2 and 3. The power grid spans approximately 7.000 km of system length, of which around 2.600 km are related to 380 kV, 3.200 km to 220 kV and 1.200 km to 110 kV voltage levels.

To investigate the propagation of voltage sags through the grid when defining a grid disturbance, such as a short circuit, the complete short circuit calculation method has been chosen, as introduced in subsection 3.2. There is no need for a dynamic RMS or EMT simulation (see subsection 6.2.2) for this type of investigation. In this case they don't provide any crucial advantages over short circuit calculation methods, but are more resource and time consuming and demand a higher level of accuracy of the grid model to achieve satisfying results.

The simulation scenarios have been limited to bolted 3-phase short circuits, which represent worst case scenarios in terms of voltage sag depth. In addition to that, only individual incidents – not multiple faults – are examined. Different scenarios are defined by varying the fault location. A typical loading scenario based on actual loading data has been chosen. Short circuits are defined at the 380 kV, 220 kV and 110 kV voltage levels. At each voltage

level, individual fault incidences are simulated for all relevant substations. The remaining voltages of the substations are noted and categorized per voltage level or grid for every simulation scenario considered.

3.5.2 Simulation Results

Following the results of simulations performed are shown for each voltage level. Because the three 110 kV grids are not interconnected with each other, they are analyzed separately. Results of all short circuit simulations of a certain voltage level or 110 kV grid are categorized in remaining voltages at the substations. Each bar graph (Figure 3.4, Figure 3.6-Figure 3.9) illustrates how many of the total substations of each voltage level or 110 kV grid are facing a certain voltage dip depth on average. When performing short circuit simulations, the number of substations of each grid affected by a certain voltage dip depth is noted and rated based on the number of substations of each grid (see Table 3.16) to obtain an average percentage for each category. Summing up the average percentages of affected substations of a certain grid category does not equal 100 %, because the voltage category for u>0.9 pu is not shown in the plots. This kind of illustration also presents how a fault event of a certain voltage level influences remaining voltages of other voltage levels. Table 3.16 lists the number of substations per voltage level or 110 kV grid.

Table 3.16: Number of substations per voltage level or grid

Grid	**Number of Substations**
380 kV	25
220 kV	52
110 kV grid 1	43
110 kV grid 2	54
110 kV grid 3	30

Figure 3.4 displays the results of faults simulated at the 380 kV voltage level. It can be seen that only very few substations are facing severe voltage sags. This means that the voltage is built up rather quickly within the 380 kV grid. Most 380 kV substations (63.1 %) have voltages above u=0.9 pu. Lower voltage levels are affected by the faults as well, although the remaining voltages are very rarely lower than u=0.6 pu. Because of the fact that the 110 kV grids are denser meshed with shorter distances between substations than the 380 kV or 220 kV grid, once they are facing a lower voltage at one of the interconnection points to higher voltage levels, most of the substations have similarly low remaining voltages throughout the densely meshed grid.

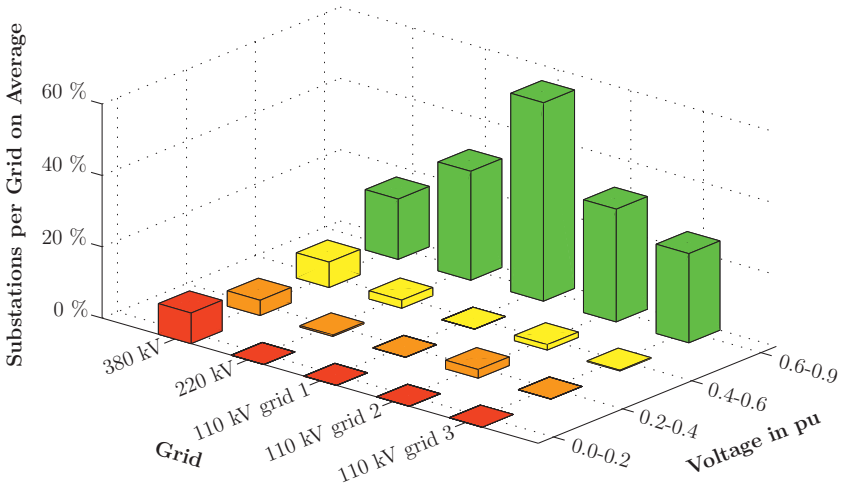

Figure 3.4: Remaining voltages for faults at the 380 kV voltage level

In Figure 3.5 the remaining voltages and hence the propagation of voltage sags after a fault at a 380 kV substation are illustrated utilizing a colored overlay. A fault at this substation represents the worst case scenario in terms of number of neighboring substations affected by severe voltage sags within the 380 kV voltage level. The colored overlay indicates the substation voltages immediately after the short circuit, ranging from red (remaining voltage u<0.2 pu) to dark green (remaining voltage u>0.9 pu), as shown in the legend below the figure. Uncolored substations are either not connected (open circuit breaker) or out of service. This figure illustrates once again how confined the propagation of severe voltage sags in such a grid structures is.

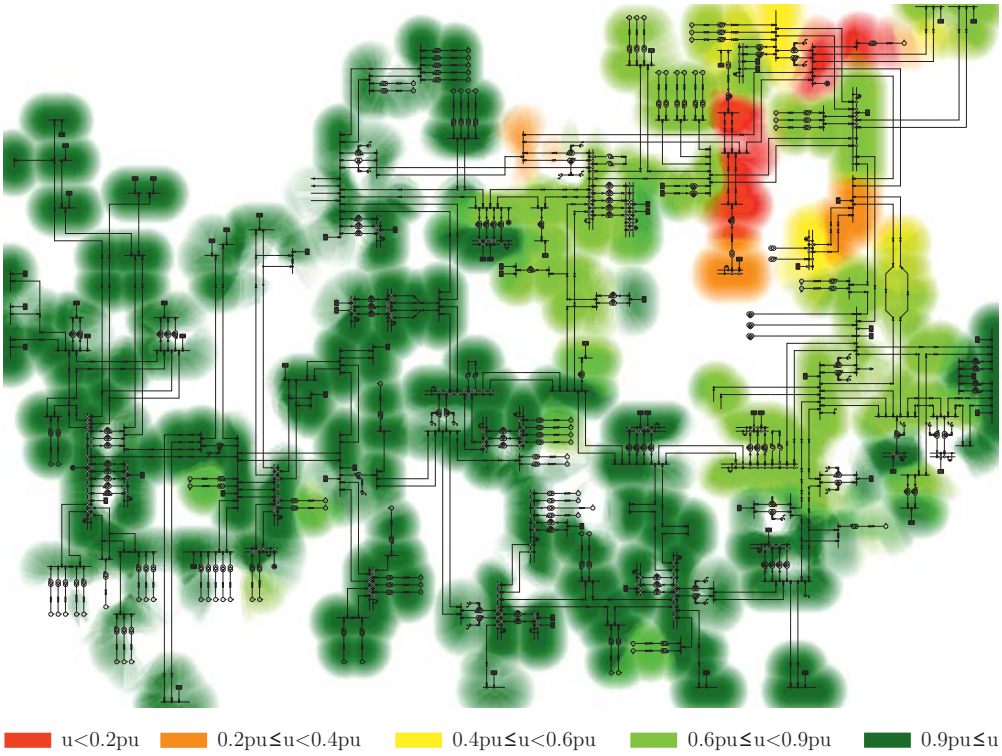

Figure 3.5: Remaining voltages after a fault at a 380 kV substation

Results for 3-phase short circuits in the 220 kV voltage level are shown in Figure 3.6. For this voltage level the same things apply as for the 380 kV level. Remaining voltages build up rather quickly, which means that only very few 220 kV substations (5 %) are facing voltages below u=0.4 pu. It can also be seen that faults hardly propagate upwards to a higher voltage level. Only 380 kV substations in the immediate surroundings of the fault location at the 220 kV voltage level are affected and even then mostly in the voltage range of 0.6 pu u < 0.9 pu.

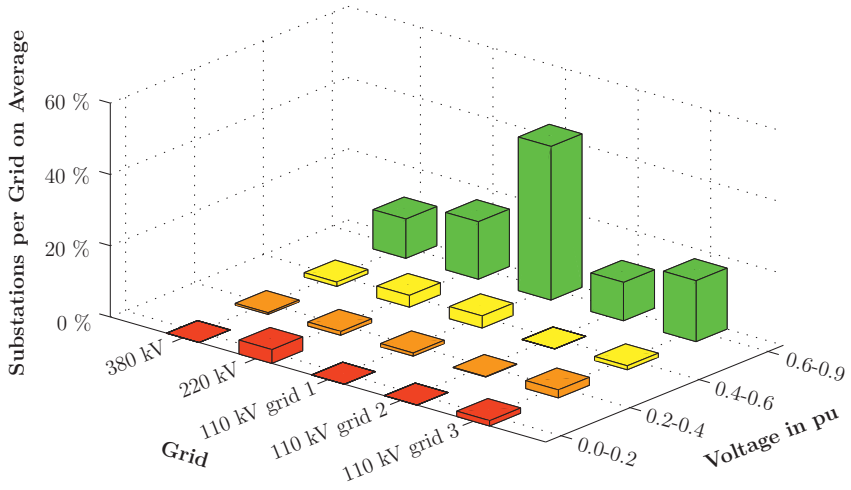

Figure 3.6: Remaining voltages for faults at the 220 kV voltage level

In Figure 3.7 results for faults in 110 kV grid 1 are illustrated. Once again it can be seen that faults from lower voltage levels scarcely propagate up to higher voltage levels. Besides, the fault incidents are barely notable in the other 110 kV grids, because there are no direct interconnections between them.

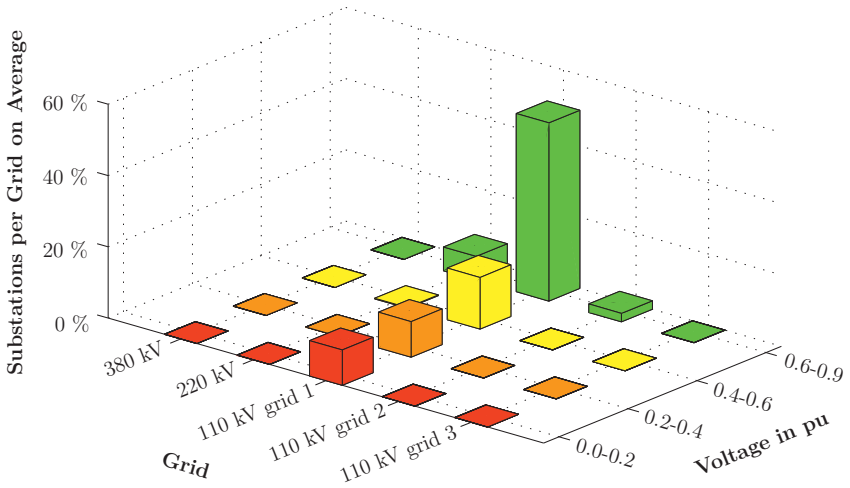

Figure 3.7: Remaining voltages for faults in the 110 kV grid 1

The 110 kV grids 1 and 2 share one 220 kV busbar. This is why they influence each other slightly. In Figure 3.8 it looks like as though grid 2 had a bigger influence on grid 1 than vice versa. This is because the structure of grid 1 is such, that the voltage is more homogenous than compared to grid 2. This means that if the voltage at the shared 220 kV busbar is lower due to a fault in grid 2, the vast majority of substations in grid 1 experiences a drop in voltage.

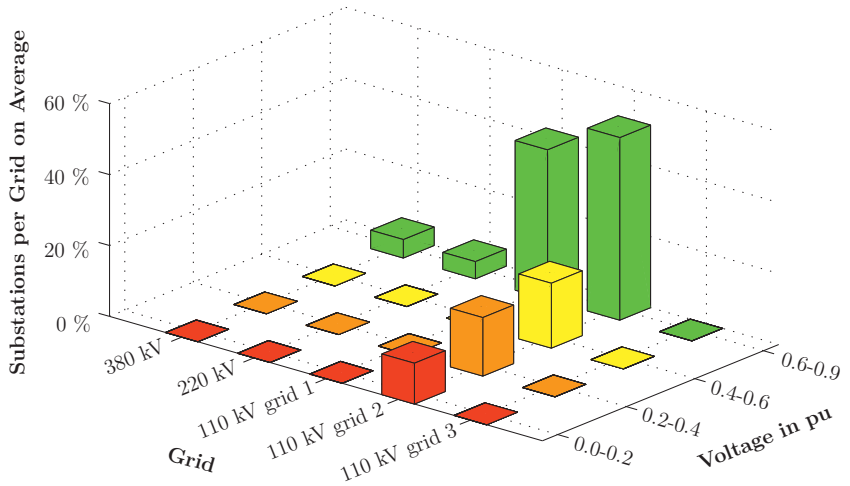

Figure 3.8: Remaining voltages for faults in the 110 kV grid 2

Figure 3.9 displays results for faults in 110 kV grid 3. This grid is even smaller with shorter lines between the substations. Therefore, faults propagate rather easily through the grid.

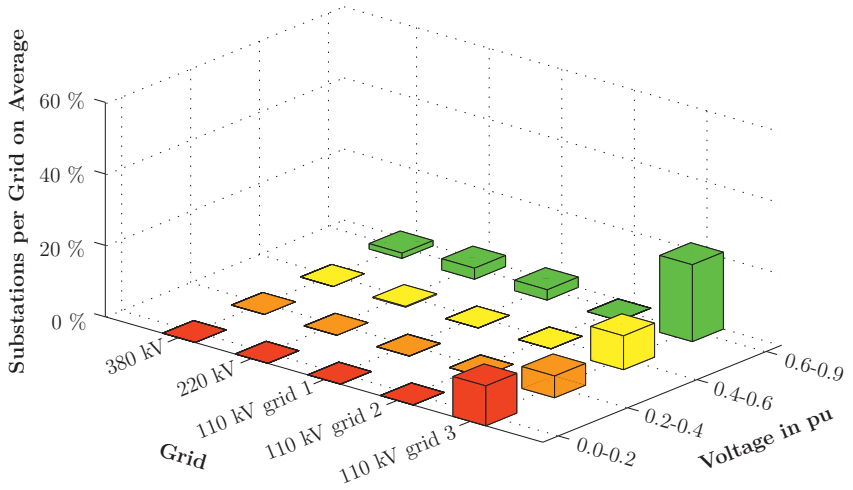

Figure 3.9: Remaining voltages for faults in the 110 kV grid 3

As expected, the results show that the higher the voltage level where the fault incident occurs, the more severe the voltage sags and the further they propagate through the grid. Results for faults at the 110 kV voltage level show that low voltages are confined to small areas. Simulating a fault at even lower voltage levels (e.g. 30 kV), the area where the remaining voltage is very low is limited to an even smaller local area and not noticeable at higher voltage levels. So faults tend to propagate downwards the voltage levels, but not upwards. This is because faults in lower voltage levels do not cause significant voltage drops in higher voltage levels, as the impedance of the transformer(s) between them is large enough to considerably limit the influence on higher voltage levels. Even for a worst case fault – a bolted 3-phase short circuit at a 380 kV busbar – the voltage sag does not affect a big area of the grid, but is more or less a local problem in a grid structure like given here. Especially when considering very low remaining voltages, e.g. below u=0.4 pu, this holds even more true.

3.5.3 Influence of Reduced Short Circuit Power

Following the current trend of increasing penetration of generation by renewables, predominantly wind power plants and photovoltaics, the short circuit power of future grids is likely to be lower when compared to the current state, especially when considering that conventional generation units with high short circuit power are replaced by renewables with low short circuit power. To investigate the influence of reduced short circuit power, the short circuit power of all generation units and external grid elements at the 380 kV, 220 kV and 110 kV voltage levels of the Central European power grid introduced in

subsection 3.5.1 and all its neighboring countries is reduced down to 10 % of its nominal short circuit power. Such a drastic reduction in short circuit power seems quite unrealistic in a foreseeable future, but was chosen as means of showing the influence of such a reduction. Besides, first investigations have shown that only slightly reducing the short circuit power of generation units and external grid elements has just a marginal influence on simulation results. Other than that, the grid structure remained exactly the same, because the point is to investigate the influence of reduced short circuit power due to non-conventional generation technologies only, not the impacts of grid reinforcements or restructuring as well.

The following tables give an overview of selected substations of each voltage level comparing their short circuit power levels before and after reducing the short circuit power of generation. The order of substations of each voltage level is random and not related to the numbering of other voltage levels' substations.

Table 3.17: Short circuit power levels of selected 380 kV substations before and after reducing generation's short circuit power

Substation	**Initial state**	**Reduced SC power**	
	GVA	GVA	%
SS 380.1	20.9	13.54	64.8
SS 380.2	9.55	7.54	79.0
SS 380.3	27.45	20.85	76.0
SS 380.4	14.05	9.42	67.0
SS 380.5	8.22	5.26	64.0
SS 380.6	15.38	9.72	63.2

Table 3.18: Short circuit power levels of selected 220 kV substations before and after reducing generation's short circuit power

Substation	**Initial state**	**Reduced SC power**	
	GVA	GVA	%
SS 220.1	12.85	8.25	64.2
SS 220.2	13.15	9.48	72.1
SS 220.3	5.32	4.23	79.5
SS 220.4	6.20	4.48	72.3
SS 220.5	14.88	7.96	53.5
SS 220.6	2.26	1.66	73.5

Table 3.19: Short circuit power levels of selected 110 kV substations before and after reducing generation's short circuit power

Substation	**Initial state**	**Reduced SC power**	
	GVA	GVA	%
Grid 1 SS 110.1	2.96	2.30	77.7
Grid 1 SS 110.2	2.04	1.15	56.4
Grid 1 SS 110.3	1.49	0.91	61.1
Grid 1 SS 110.4	2.95	1.85	62.7
Grid 2 SS 110.1	0.98	0.70	71.4
Grid 2 SS 110.2	1.28	1.05	82.0
Grid 2 SS 110.3	2.18	1.58	72.5
Grid 2 SS 110.4	2.76	2.16	78.3
Grid 2 SS 110.5	1.58	1.05	66.5
Grid 3 SS 110.1	1.08	1.01	93.5
Grid 3 SS 110.2	3.63	2.94	81.0
Grid 3 SS 110.3	4.55	3.28	72.1
Grid 3 SS 110.4	3.21	2.61	81.3
Grid 3 SS 110.5	2.88	2.40	83.3

It can be seen that even when reducing the short circuit power of all generation in the 380 kV, 220 kV and 110 kV voltage levels to 10 % of their original short circuit capacity, the short circuit power levels at substations throughout the voltage levels do not seem to drop as significantly. As the tables above indicate, mostly they remain at around 70 % of their original state values. This can be attributed to the fact that the short circuit impedance is mainly dictated by the grid structure, which remained unchanged in both scenarios.

Simulations regarding voltage sag propagation have been performed for the 10 % short circuit power scenario as well. As expected, more substations were affected by low remaining voltages, which means the area of low voltages was bigger when compared to the initial scenario. But still, the remaining voltages were mostly in the same range, as shown in Figure 3.10 by means of exemplary results of the 380 kV voltage level simulations. The figure illustrates the increase in the number of average substations affected by a certain remaining voltage when reducing the short circuit power of generation compared to the original state (as shown in Figure 3.4). Results of other voltage levels look similar and are therefore not shown here explicitly.

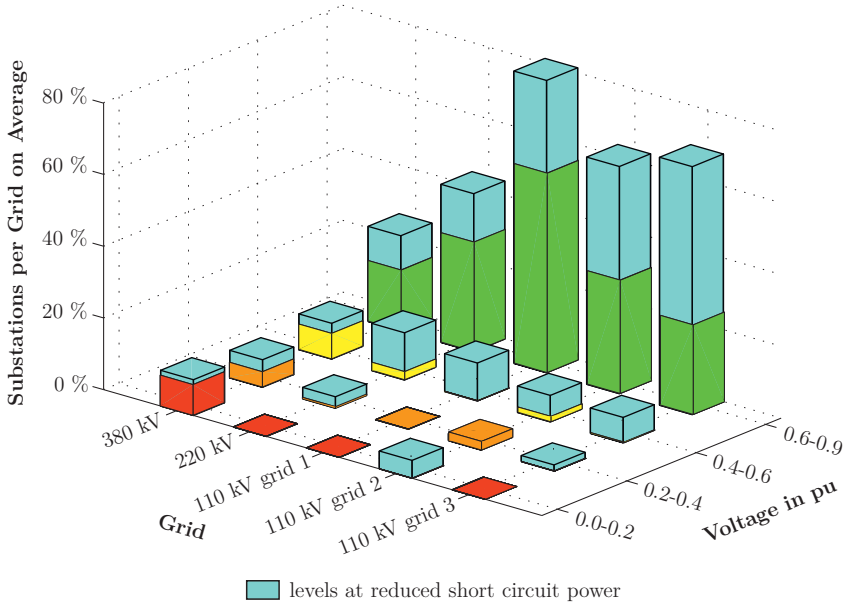

Figure 3.10: Remaining voltages for faults at the 380 kV voltage level before and after reducing short circuit power

3.6 Conclusion

Fault and voltage dip statistics of different regions within Europe and also overseas countries were presented. Although the data origin is quite diversified, the statistics are similar throughout most regions. For example, most of the fault events (around 80 %) are cleared within 200 ms and at least 72 % of all fault events have been registered with a remaining voltage during the fault above u=0.8 pu. It was shown that there are very rarely fault events, where the remaining voltage is very low and the fault duration is longer than 200 ms.

Similar results for remaining voltages throughout a power grid have been shown by means of short circuit simulations on an actual Central European power grid. It has been demonstrated that even at high voltage levels, the voltage sags are very limited, both in terms of voltage dip depth and also in the area affected by severe voltage sags. This means that only a few power plants would face serious low voltages that could endanger proper operation of their units. One has to keep in mind, that the worst case scenario has been considered when simulating bolted 3-phase faults (no fault impedance), which are very rare, statistically speaking, as shown in subsection 3.3. So in reality the vast majority of the time voltage sags following grid disturbances are even less severe than performed in the simulations, hence remaining voltages would be higher, even directly at the fault location.

The influence of a possible reduction of short circuit power in future grids was investigated by performing simulations on a Central European power grid. Results have shown, that

even when reducing the short circuit power of all generation in high voltage system levels down to 10 % of its original value, the short circuit power levels of substations throughout the grid didn't drop as drastically. As a consequence, the remaining voltage levels didn't change significantly either. Keeping in mind that such a reduction of the overall short circuit power installed might not be reasonable in a foreseeable future, the increasing penetration of renewable energy sources should not have a big influence on short circuit power levels throughout the grid and with it on the voltage sag propagation in grid structure like given here.

Rare combinations of circumstances that could produce system instability, can always occur in any system. Designing demands for FRT capabilities of power generation units based on such extreme conditions might not be practicable though. Especially if different extreme conditions are required simultaneously, a lot of power generators might have difficulties maintaining synchronism. Thus, it's important that FRT requirements are reasonable. Unreasonable combinations of requirements such as retaining a very low voltage for a prolonged fault duration at an unfavorable operating point of the power generation unit might lead to FRT requirements that may not be met by a lot of commercially and technically viable equipment. [19]

Connection requirements for generators by ENTSO-E [4] and national grid codes require power generation units to ride through voltages as low as u=0.05-0.3 pu or even lower for a period of around 150-250 ms. Given that such low voltages rarely occur or if so, are very limited to a local area – as indicated by simulations – those requirements might be too restrictive in terms of the capability to ride through faults. Hence they might deny the grid connection of certain power generation units that might be fine riding through faults at – statistically speaking more likely – higher remaining voltages. Nonetheless, LVRT-requirements are an important means to ensure proper operation of power generation units during grid disturbances, so that they do not disconnect from the grid when facing the slightest disturbances.

4 LVRT Testing

This section covers topics regarding LVRT testing. Basic LVRT capability test methods are presented. Regarding LVRT test equipment, the focus in this thesis lies on an impedance based voltage divider. An equipment testing standard by the IEC using this test method is provided in subsection 4.3. Subsequently, the procedure for certifying power generation units for their LVRT capability is discussed. In particular, the certification through validated simulation models of power generation units is presented based on a case study, where gas-engine driven units had to be certified, in order to be allowed to be connected to the German power grid.

4.1.1 Introduction

Due to the increasing and no longer negligible number of decentralized power plants in recent years, gird connection requirements and guidelines have been introduced for these units worldwide. Among other things, these connection codes state that generation units are required to support the grid during grid disturbances and are only allowed to be disconnected from the grid under certain circumstances. Those requirements specifying the LVRT capability of a generation unit are defined through voltage-against-time-curves. An overview of different LVRT curves from various countries is given in Figure 4.1. Generation units are generally allowed to be disconnected from the grid, if the voltage – usually specified at the connection point – drops below the given voltage-against-time-curve.

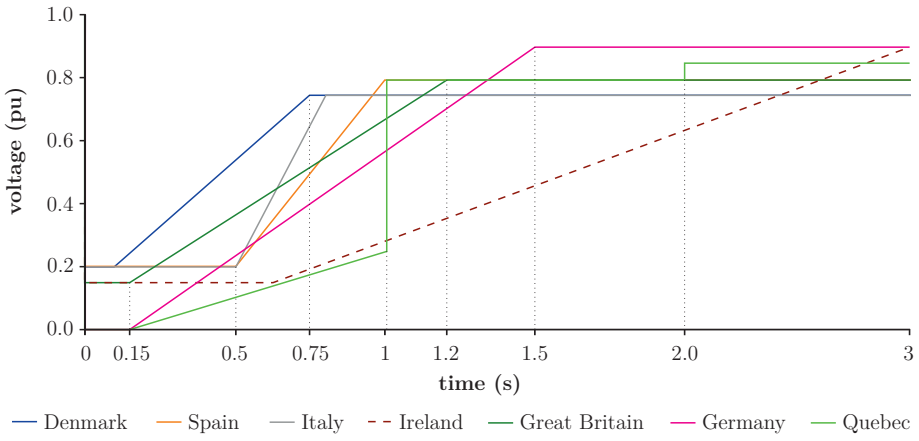

Figure 4.1: Comparison of various LVRT curves of different countries' grid codes [30]

As can be seen, the LVRT curves can differ quite a lot – mainly in remaining voltage and fault duration – depending on the grid code. It has to be noted that by far not all grid

codes' LVRT voltage profiles are shown here. Constantly new grid codes and connection requirements are emerging or old ones are being updated, so it's quite difficult to keep track of them all or more important, to establish the LVRT capability of a certain generation unit for all countries. Only country or grid code specific LVRT capability tests can be performed. Besides, the validation and certification process can vary too, depending on the issuing country.

4.2 LVRT Capability Test Methods

There are several test methods to emulate a fault event. They can be divided into four different types of voltage sag generators:

- synchronous generator with fast voltage control
- series/shunt impedance forming a voltage divider
- tap changing transformer
- full power converter

In Figure 4.2 the principle of these four basic methods is provided.

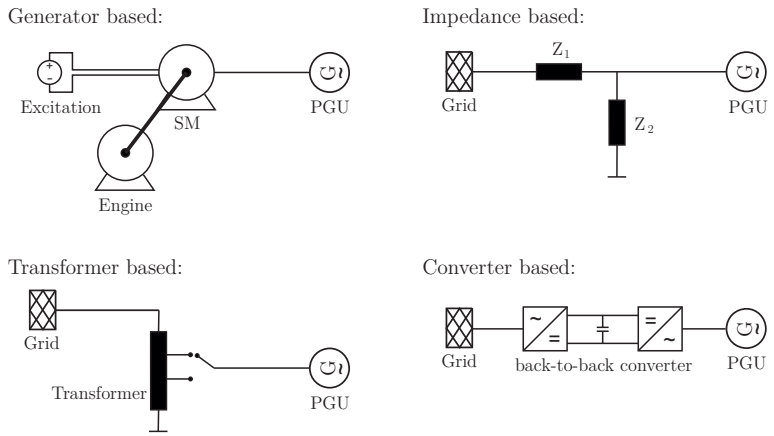

Figure 4.2: Overview of different types of voltage sag generators [37, 38]

4.2.1 Synchronous Generator with Fast Voltage Control

In the generator based approach a diesel powered synchronous generator produces controlled symmetrical voltage sags by changing the field excitation. Hardware costs are high due to the weight and scale of the diesel engine and the synchronous generator. Only symmetrical faults can be emulated with this test method. Besides, ramp-up and ramp-down times are within several cycles of mains frequency, which is too slow to emulate realistic grid faults.

4.2.2 Shunt Impedance Voltage Divider

Shunt impedance based voltage sag generators create voltage dips by switching an impedance in parallel to the line. This is utilized by switching of impedances of an impedance bank. An additional impedance is connected in series to limit the short circuit current and the influence on the feeding grid. In addition to that, the short circuit power can be adjusted by varying the value of the series impedance to emulate connection points with low short circuit power. A by-pass connection of the series impedance may be applied prior and after the voltage dip test. This test method allows for emulating 1-phase, 2-phase and 3-phase faults of variable dip depth and length. It is very easy to implement and low in cost. However, there is the risk of over-voltages caused by switching transients.

4.2.3 Tap Changing Transformer

Transformer based voltage sag generators are composed of a step-down auto-transformer with on-load tap changer (OLTC). The voltage dip depth is adjusted by an appropriate tap change. Utilizing an OLTC auto-transformer is a suitable solution for building a low cost voltage sag generator. However, to emulate 3-phase faults phase individually controlled tap changers are needed.

4.2.4 Full Power Converter

A back-to-back converter connected between the grid and the power generation unit builds a full converter based voltage sag generator. This configuration has the best performance in terms of controllability and programmability. Disadvantages of this solution are high hardware costs, complexity of control and its limitations due to limited overvoltage and overcurrent capabilities, which is essential for dynamic simulation studies applying grid faults. [37–39]

4.2.5 Other Methods

Of course other solutions than the four presented ones to create voltage sags are possible. Reference [40] introduces a voltage dip generator, which utilizes an inductive divider consisting of a series impedance and a parallel branch, where a tap transformer and an impedance is located. In [41] a 3-phase induction generator with a control mechanism to modify its shaft position is presented. If voltage adaption is needed, tapped transformers are implemented. The operation is controlled by a programmable logic controller. This way any voltage-time profile is programmable, not just rectangular ones. A 4-wire matrix converter based voltage sag generator is discussed in [37]. It has basically the same

characteristics as the above mentioned full converter solution, but modulation algorithms are not as complex.

4.3 Equipment Testing Standard

The main purpose of the IEC 61400-21 ed2.0 standard [39] is to provide a uniform methodology to ensure consistency and accuracy in the presentation, testing and assessment of power quality characteristics of grid connected wind turbines. The standard provides, amongst other things, an LVRT testing procedure and test setup. Although the standard is addressing wind turbines, the methodology is widely accepted for power generation units other than wind turbines, as many papers and guidelines confirm. Figure 4.3 shows the voltage sag generator given by the standard.

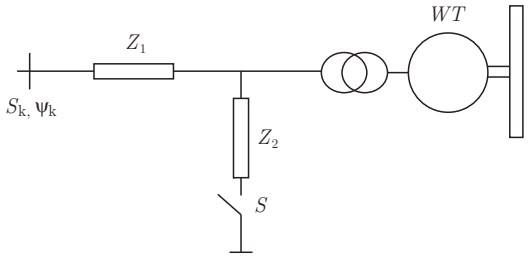

Figure 4.3: Short circuit emulator for wind turbine testing from IEC 61400-21 [39]

According to the standard the impedance Z_1 is for limiting the effect of the short circuit on the external grid. The size of the impedance should be selected, so that the testing procedure is not causing an unacceptable situation at the external grid and at the same time not significantly affecting the transient response of the wind turbine. A specific short circuit power is not given and may be agreed between the manufacturer, equipment test crew and utility. It has to be noted in the test report though. The voltage drop is created by connecting the impedance Z_2 by closing the switch S. The combination of Z_1 and Z_2 determines the remaining voltage during the dip. This value is defined for the power generation unit not connected, in order to eliminate the influence of the equipment under test (EUT). This way the same voltage dip test can be applied to different test objects without changing the settings of the test setup, unless there's a need for adapting the short circuit ratio. [39]

It has to be noted, that some grid codes and technical guidelines basically refer to the standard IEC 61400-21 ed2.0 [39], but defining differing test conditions. Mostly, the procedure is the same as outlined in the standard, but short circuit ratio, voltage dip profiles and tolerances might be defined independently. For example the technical guidelines for testing and validating the LVRT capability of power generation units by the

FGW Germany [42] do not consider voltage levels at generator terminals after switching in the series impedance of the test container. It is only stated that the power generation unit should be able to operate permanently within a voltage range of 0.9 pu u 1.1 pu at the point of common connection (PCC) without disconnecting. [42, 43]

4.4 Validation of LVRT Simulation Models of Decentralized Power Plants

In order to simulate the real life behavior of decentralized power plants during fault events, accurate simulation models have to be established. Undergoing a certain validation process, such simulation models are checked by test bodies. If the validation procedure is successful, the checked power generation units receive a certificate stating their LVRT capability. In this subsection a simulation model is discussed, which was built to satisfy the requirements given by the German entity "Bundesverband der Energie- und Wasserwirtschaft" (BDEW[6]). A validated simulation model allows a specific set of generation units to be connected to the German power grid. The power systems analysis software used for this study was DIgSILENT PowerFactory.

4.4.1 Certification Procedure

In Germany the technical guideline "Generating Plants Connected to the Medium-Voltage Network – Guideline for generating plants' connection to and parallel operation with the medium-voltage network" was issued by BDEW in June 2008 [43]. Power generation plants complying with the technical guidelines can apply for a certificate at specific certification centers. Such a certificate qualifies the unit to be connected to Germanys MV network. Since 01.01.2014 combustion engine powered generation units are obligated to have a certificate in order to be allowed to connect to the German power grid [44]. The guideline is only applicable to newly installed power generation units or units, where significant changes have been made, such as repowering.

The technical guideline differentiates between power generation units and power generation sites. A power generation unit is a single unit generating electrical power. A power generation site is a set of one or more power generation units including auxiliary equipment. The definitions used in the technical guideline are illustrated in Figure 4.4.

[6] German Association of Energy and Water Industries.

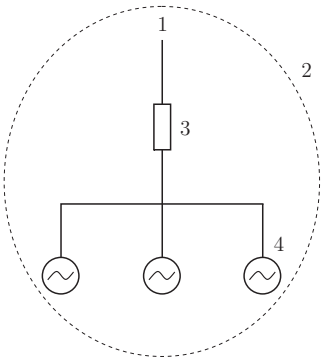

1 Point of common coupling

2 Power generation site

3 Connection installation (cables, transmission station)

4 Power generation unit

Figure 4.4: Terms and definitions used in the technical guideline [43]

Every power generation unit is required to have a unit certificate. This certificate confirms that the power generation unit complies with the technical guidelines laid out by the BDEW. An additional certificate for the power generation site is needed, if the total power of the site exceeds S=1 MVA. This site certificate can be requested in a separate certification process. In order to be able to apply for a site certificate, it is mandatory that all power generation units within the site have a unit certificate. [43]

A brief overview about the certification process is given in Figure 4.5.

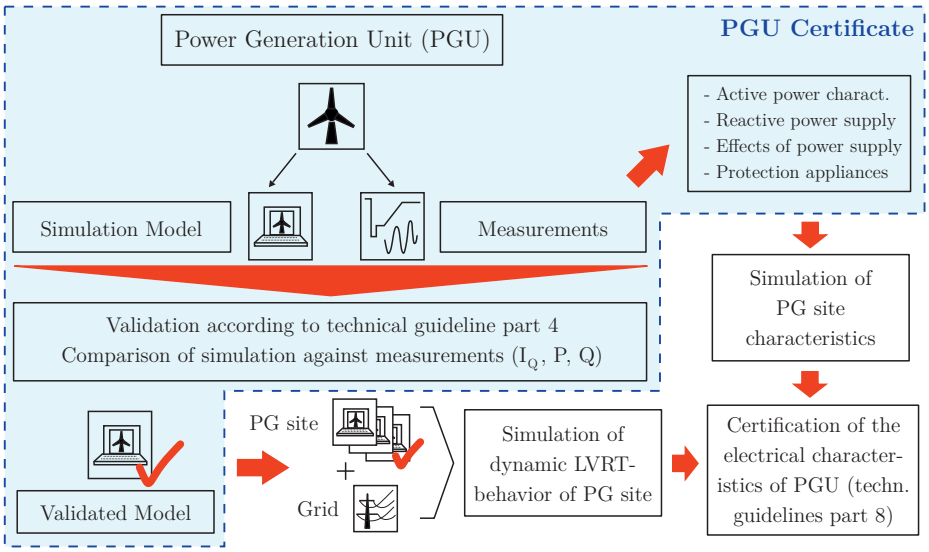

Figure 4.5: Overview of certification procedure [45]

As can be seen, there are two options to get a unit certificate: the power generation unit can either be tested on-site or by performing simulations of validated simulation models. The big advantage of validated simulation models is that not only the simulated power

generation unit gets certified, but also all units of same type within a nominal power range P_n given in equation (4.1) [43].

$$1/\sqrt{10} \cdot P_n' \leq P_n \leq \sqrt{10} \cdot P_n' \tag{4.1}$$

Here P_n' is the nominal power of the simulated power generation unit. This way a range of generation units of the same type each receive a unit certificate by validating one simulation model. Besides, testing the whole range on-site is time consuming and costly. That's why the certification process with a validated simulation model is preferred in most cases over testing all power generation units separately. The following subsection covers the validation process of simulation models.

4.4.2 Validation of Simulation Models

The technical guidelines by "Federation of German Windpower and other Renewables – FGW" give instructions for the measurement and test procedures, the evaluation of measurements and requirements regarding modeling, validation and certification. Part 4 of the technical guidelines covers the requirements concerning the modeling and validation of simulation models [27]. In order to get validated, the simulation model has to be able to represent certain electrical quantities with a given accuracy. According to the guidelines, simulation results for active power, reactive power and reactive current are compared to measurements for validation. Measurements and simulation results are divided into categories depending on the switching events. Each of these categories is divided into two sub-categories, namely a transient and stationary area. In every segment of data, simulation results have to be within a given range of deviation from measurement data. Figure 4.6 illustrates the allocation of transient (orange) and stationary (blue) areas using a reactive power measurement data as an example.

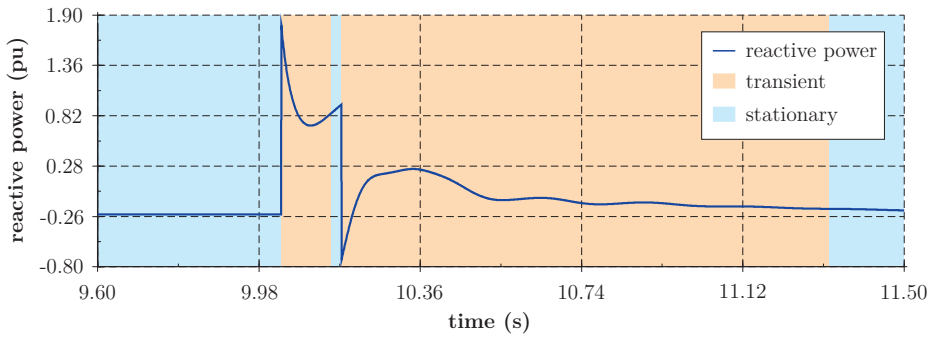

Figure 4.6: Allocation of transient (orange) and stationary (blue) areas using the exmaple of reactive power measurement data

Several pre-defined simulation scenarios have to be validated. They vary in voltage dip depth (given at the PCC), fault clearing time and operating point of the machine (i.e. remaining voltage at the PCC of u=0.3 pu for t=150 ms, power factor pf=0.95 ind., half load). Aside from 3-phase faults, 2-phase and 1-phase faults have to be addressed in the validation process as well.

4.4.3 Case Study

The simulation model should be able to represent the electrical behavior – namely active power, reactive power and reactive current – of a power generating unit according to the technical guidelines as accurate as possible. There are two basic transient simulation methods: the instantaneous value simulation (EMT – Electro-Magnetic Transients) and the transient stability simulation (RMS – Root Mean Square). In EMT-simulations, the machine's flux and stator voltage equations are represented without simplifications. Therefore, dc components as well as harmonic components in short circuit currents and generator torque are represented in simulation results. In contrast, using the RMS simulation method, the machine's stator voltage equations get simplified (stator flux transients neglected). For this reason, fundamental frequency oscillations are not shown in simulation results. Nonetheless, the RMS method is required to be used by the technical guidelines [27]. The same simulation model can be used for different motor-generator sets. Therefore, only by parametrizing the simulation model a wide range of units can be covered for certification. The generator's power input is assumed to be constant throughout the simulation.

4.4.4 Simulation Setup

The grid topology used for simulations corresponds to the actual test setup used for measurements and is shown in Figure 4.7.

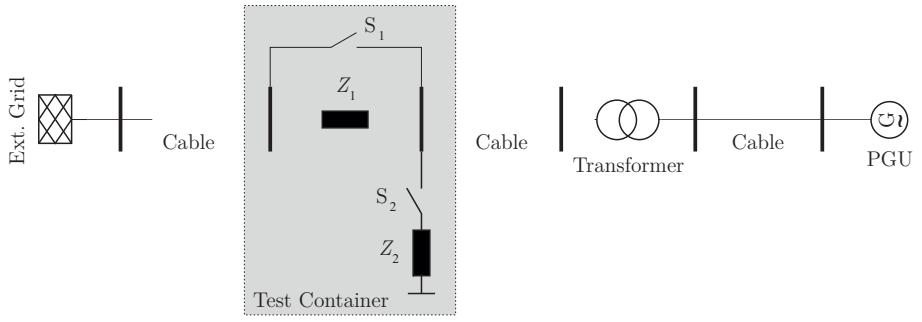

Figure 4.7: Grid topology used for validation

The LVRT test container (see subsection 4.2 and 4.3 for further details) is a widely accepted method for performing LVRT capability tests for validation and certification purposes. The series impedance Z_1 limits the influence of the test procedures on the external grid. The shunt impedance Z_2 is adjusted to achieve a certain remaining voltage at the PCC during the fault event. The impedances (air-core coils) can be switched through circuit breakers. The desired remaining voltage is set up through the voltage divider defined by the shunt impedance Z_2 without the EUT connected.

A typical test procedure looks like this:

Test setup

1. Disconnecting the EUT
2. Adjusting the series impedance Z_1 according to the expected short circuit current
3. Adjusting the shunt impedance Z_2 to achieve a certain voltage drop at the PCC
4. Impedance switching states: Series impedance Z_1 is bypassed by closing its circuit breaker, shunt impedance Z_2 is disconnected by opening its circuit breaker.
5. The EUT is reconnected and run up to the desired operating point

Test run

6. Switching in of series impedance Z_1 (opening its circuit breaker)
7. Initiating the fault event by switching in of shunt impedance Z_2 (closing its circuit breaker)
8. Clearing the fault by disconnecting the shunt impedance Z_2 (opening its circuit breaker)
9. Disengaging the series impedance Z_1 (closing its circuit breaker)

The generation units under study are synchronous machines with an excitation system using a rotating rectifier. The structure for the excitation system is based on the IEEE standard 421.5 for excitation system models [46]. An automatic voltage regulator (AVR) is used as voltage regulator. Within a given voltage range of 0.9 pu $< u <$ 1.1 pu it keeps the power factor constant. Outside of this voltage band it acts as voltage regulator.

The model used for simulations is based on the IEEE AC8B model for AC supplied rectifier excitation systems [46] and is shown in Figure 4.8. All relevant parts and signals are highlighted and named as well. Input and output signals are shown in orange, controller parts in green and excitation system characteristics in blue.

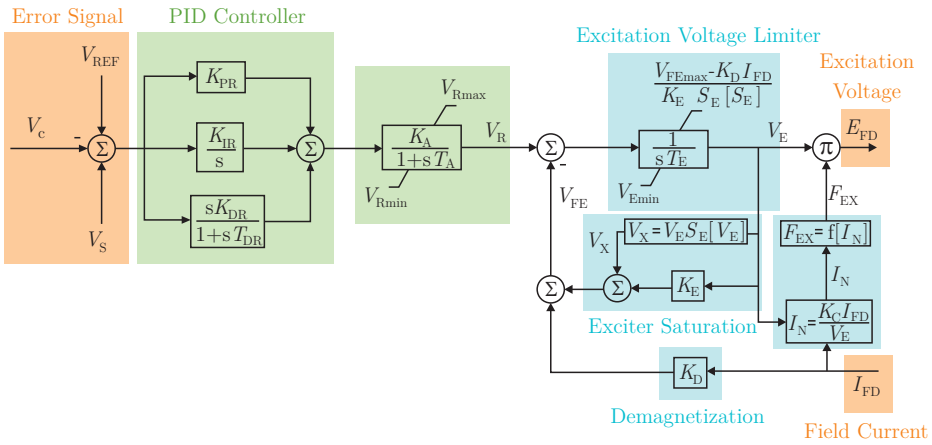

Figure 4.8: Excitation system model IEEE AC8B

For validation purposes though, this representation of the excitation system is too vague and yields simulation results far outside the allowed tolerance for simulation error. That's why the model had to be adapted in close collaboration with generator and voltage controller manufacturers, in order to be able to replicate the excitation system in the simulation model as closely as possible.

4.4.5 Simulation Results

Simulation results and analyses of one specific test are shown as an example. Aside from the three quantities active power, reactive power and reactive current – as required by the technical guidelines – the voltage characteristic is shown, but not used for validation purposes. In addition to simulation and measurement data of the terminal voltage, switching events of the series and shunt impedances are displayed in Figure 4.9 (obviously the events apply to the other figures as well). Test results shown in Figures 13-16 were performed on a S_n=785 kVA machine at half load and with a power factor of pf=0.85 ind. The fault event was defined with a remaining voltage of u=0.3 pu and a fault clearing time of t=150 ms.

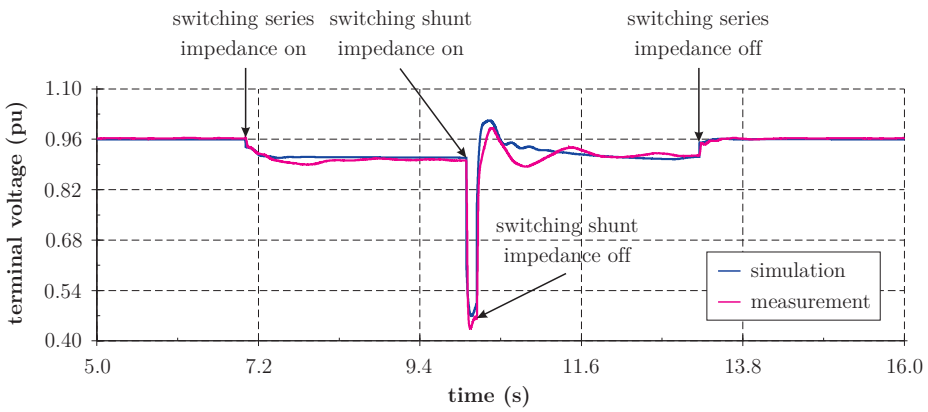

Figure 4.9: Terminal voltage – Simulation (blue) and measurement (magenta)

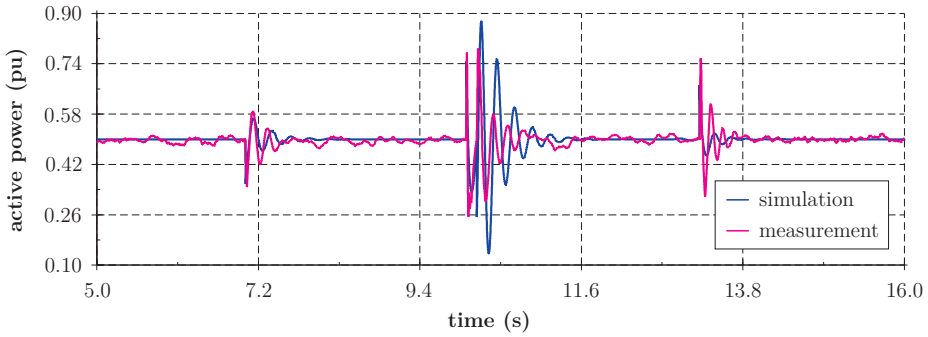

Figure 4.10: Active power – Simulation (blue) and measurement (magenta)

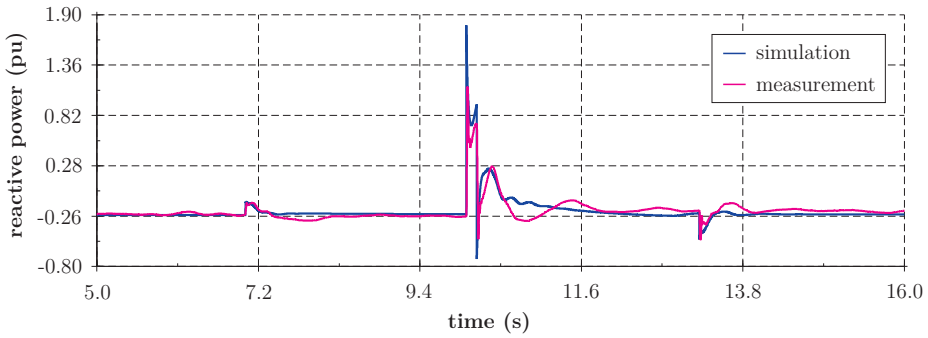

Figure 4.11: Reactive power – Simulation (blue) and measurement (magenta)

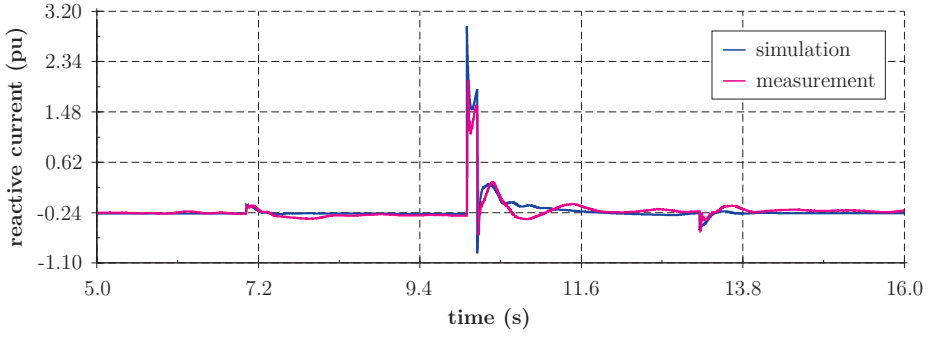

Figure 4.12: Reactive current – Simulation (blue) and measurement (magenta)

As previously mentioned, the data is divided into transient and steady state areas, so that simulation deviations within those areas can be calculated. The areas relevant for the validation process are highlighted in Figure 4.13, using reactive power characteristics as an example, although the same areas apply to active power and reactive current also. The areas are defined based on measurement data. The area before area "A 3" is not investigated in the validation process and can be disregarded.

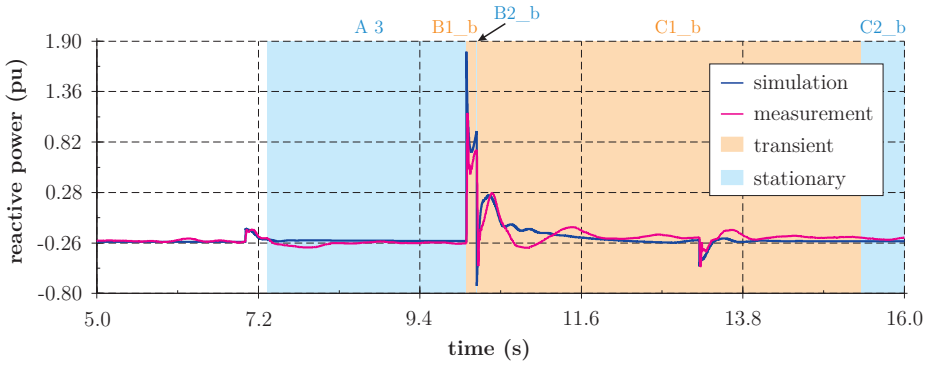

Figure 4.13: Allocation of transient (orange) and stationary (blue) areas

Corresponding to the time characteristic of reactive power shown in Figure 4.13, the evaluation of simulation errors is given in Table 4.1. It shows the time stamps of each area, the error of mean and maximum value of reactive power and for each the permitted limit of error, as given in the technical guidelines. As can be seen, no limits have been violated and therefore, this reactive power characteristic meets the requirements given in the technical standards by FGW [27]. It has to be noted though, that the data shown in Table 4.1 is only a very small fraction of the whole data that needs to be evaluated, in order to get the simulation model validated.

Table 4.1: Evaluation of reactive power simulation errors

Area	**Start**	**End**	**ΔQ_{mean} in %**		**$\lvert\Delta Q_{max}\rvert$ in %**	
	s	s	error	permitted	error	permitted
A 3	7.300	10.030	0.59	7	1.14	15
B1_b	10.030	10.152	6.82	20		
B2_b	10.152	10.175	6.97	7	7.89	15
C1_b	10.175	15.320	5.10	20		
C2_b	15.320	20.000	0.43	7	3.69	15

4.5 Conclusion

An overview of different LVRT capability test methods has been given. Such equipment is emulating a fault event at the PCC or generator terminals in order to test the EUT for its LVRT capability. The most common test methods with all their advantages and disadvantages have been discussed. A short insight into the equipment testing standard IEC 61400-21 [39] was given, which is mentioned very often in the field of LVRT capability test equipment.

In addition to that, the validation and certification procedure was presented, as customary for power generation units to be connected to Germany's power grid. A complete excitation system model according to the requirements laid out in the technical guidelines by FGW [27] has been built, which can be used for the certification of power generation units and power generation sites. Just as import as the model structure are its parametrization and the generator data. Even though most of the data is provided through data sheets by manufacturers, parameters are subjected to tolerances, sometimes up to 40 %. Certain parameters of the generator can't be measured and therefore have to be estimated or based on other data. Another issue is the saturation data of the excitation system. Although it was given by the manufacturer as well, it had to be recalculated and corrected based on specific measurement data, in order to attain a plausible saturation curve. Due to the fact that the model parametrization has a huge impact on simulation results and with it on the model validation, achieving a set of working parameters is a similarly big challenge as developing the model structure, in order to achieve satisfying simulation results within margin of error.

A few specifications given in the technical guidelines by FGW [27] are not very clear and leave room for interpretation. This can lead to misunderstandings between the certificate issuer and the certificate candidate. In order to prevent such misunderstandings as much as possible, a close collaboration between these two parties is highly recommended.

5 Limitations of LVRT Testing

As most test methods, LVRT capability testing by means of an LVRT test container – as introduced in the previous section – has certain limitations. First, the influence of external parameters, such as the short circuit power, is investigated by performing basic simulations. Secondly, the focus lies on the impact of LVRT test equipment on the LVRT capabilities of a power generation unit during LVRT tests. Its influence is analyzed in detail and recommendations for modifications of the test procedure are given.

5.1 Introduction

Östman et al. [19] discuss the impact of different grid characteristics and grid dynamics on low voltage ride through capabilities of generators. They give an overview of factors affecting the fault ride through behavior, which are divided in electrical system factors and power generation unit specific factors:

Electrical system factors:

- Shape of the voltage dip
- Absolute level of the voltage dip
- Fault type (1-phase, 2-phase, 3-phase)
- Fault clearing time
- Fault location
- Grid strength and topology
- Active and reactive power conditions prior to the fault
- Active and reactive power requirements after fault clearance
- Load characteristics

Power generation unit factors:

- Rotating inertia
- Generator reactance
- Excitation system design
- AVR control
- Engine response and control

As already stated, this section is going to focus on electrical system factors, such as grid strength and topology. Performing LVRT tests with an LVRT test container falls into the category of changing the grid topology and with it the grid strength, since a test container

basically is a configuration of air-core coils, and therefore changing the system impedance by connecting it between the external grid and the EUT.

5.2 SCR Influence on Dynamic Behavior of EUT

A case study was performed to investigate the influence of the SCR on the dynamic behavior of a synchronous generator. The grid configuration used for this simulation is shown in Figure 5.1. It basically consists of a gas engine driven synchronous generator (data see Table 5.1), connected via cable to the low voltage side of the transformer (data see Table 5.2), which finally connects to the external MV grid via another cable. The location where the fault is simulated is also highlighted.

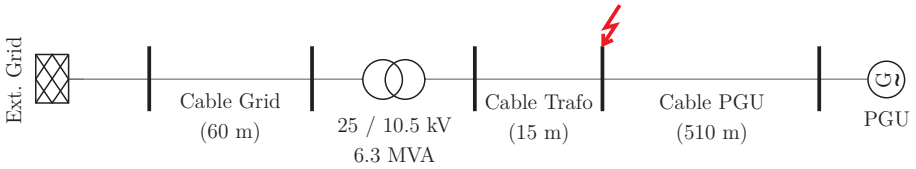

Figure 5.1: Grid setup for SCR influence case study

Table 5.1: Synchronous generator data

Parameter	Value	Unit
U_n	10.5	kV
S_n	2.492	MVA
H	0.8	MWs/MVA
x_d	1.685	pu
x_q	0.795	pu
x_d‘	0.180	pu
x_d”	0.095	pu
x_q‘‘	0.129	pu
T_d’	0.330	s
T_d”	0.031	s
T_q”	0.025	s

Table 5.2: Transformer data

Parameter	Value	Unit
U_{n1}	25	kV
U_{n2}	10.5	kV
S_n	6.3	MVA
u_k	7.83	%
P_{cu}	27	kW
I_0	0.2	%

Two different scenarios are investigated:

- Scenario 1: low SCR, weak external grid (S_k"=5 MVA)
- Scenario 2: high SCR, strong external grid (S_k"=50 MVA)

The fault event is implemented by switching a shunt impedance at the fault location. It is set to achieve a remaining voltage of u=0.05 pu (generator no-load) for a fault duration of 250 ms for this simulation. So the only thing that changes between both scenarios is the short circuit power of the external grid and with it the shunt impedance, in order to achieve a similar voltage dip depth in both cases. Side-by-side comparisons will be shown with the weak grid on the left and the strong grid on the right.

The voltage-against-time curves in Figure 5.2 illustrate that transient responses are slower in weaker grids, i.e. time constants of transients are higher.

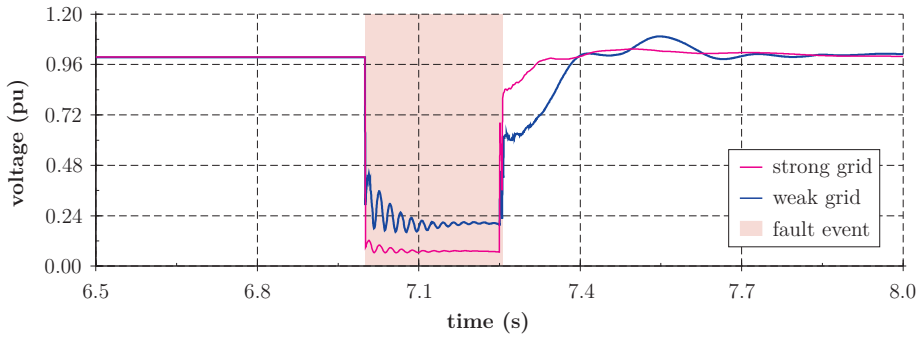

Figure 5.2: Voltage-against-time curves in a weak and a strong grid

Excursions of active power are shown in Figure 5.3. The difference in the transient behavior can be explained as follows. The synchronizing torque K_S is given by equation (5.1)[7].

$$K_S = \frac{E' E_B}{x_T} \cdot \cos \vartheta \tag{5.1}$$

Here E' is the voltage behind the transient reactance x_d', E_B the external grid voltage, ϑ the angle between E' and E_B and x_T the total impedance. Given a strong grid, the grid impedance is low, so the synchronizing torque K_S is high. This has two effects: first, it causes a higher initial overshoot and second, a faster decay of the transient oscillation, compared to a weak grid with a low synchronizing torque. Furthermore, the damping power P_D also influences the total electrical power. Machowski et al. [47] explain how the damping power P_D can be calculated. They give an approximation as shown in equation (5.2).

[7] Utilizing the classical model for generator representation given in [22].

$$P_D = V_S^{\,2} \cdot \left(\frac{x'_d - x''_d}{(x_C + x'_d)^2} \cdot \frac{x'_d}{x''_d} \cdot T''_d \cdot \sin^2 \vartheta + \frac{x'_q - x''_q}{(x_C + x'_q)^2} \cdot \frac{x'_q}{x''_q} \cdot T''_q \cdot \cos^2 \vartheta \right) \cdot \Delta\omega \tag{5.2}$$

The parameter V_S is the stator voltage, $\Delta\omega$ the rotational speed deviation from rated speed, and the other parameters are synchronous machine reactances and time constants. Parameter x_C represents the grid connection impedance. For stronger grids this connection impedance x_C is lower, which means the damping power P_D and thus the damping effect is higher. The influence of both factors, the synchronizing torque K_S and the damping power P_D, can be clearly seen in Figure 5.3.

Another aspect that can be gathered comparing the two plots in Figure 5.3 is the frequency of the transient response after clearing the fault. It looks like as though for the stronger grid the oscillation frequency were higher. This can be explained by calculating the undamped natural frequency ω_n given by equation (5.3) [22].

$$\omega_n = \sqrt{K_S \frac{\omega_0}{2H}} \tag{5.3}$$

Here ω_0 is the rated speed and H is the inertia constant. For a given setup the rated speed ω_0 and the inertia constant H are fixed constants. With varying the strength of the grid, i.e. its grid impedance, the synchronizing torque K_S is altered. So as we've already established, for a stronger grid the synchronizing torque K_S is higher, which means that the natural frequency ω_n is higher as well. This confirms the oscillatory behavior seen in Figure 5.3.

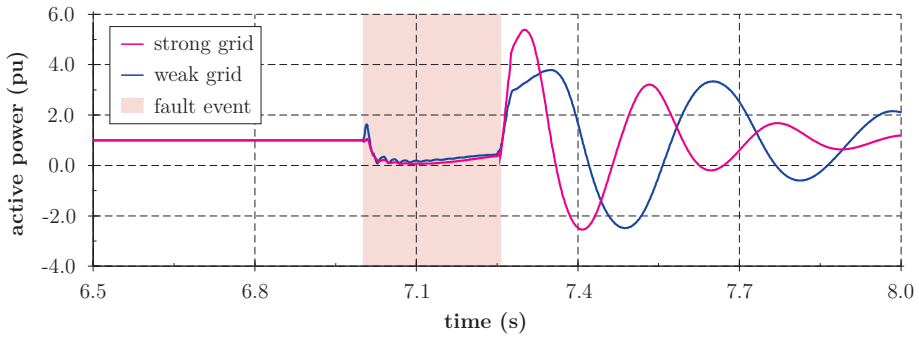

Figure 5.3: Active power excursions in a weak and a strong grid

The rotor angle excursions during and after the fault are displayed in Figure 5.4. Same things apply as to the active power excursions discussed above. What else can be seen here is that the initial rotor angle is lower for a stronger grid, which also increases the synchronizing torque K_S.

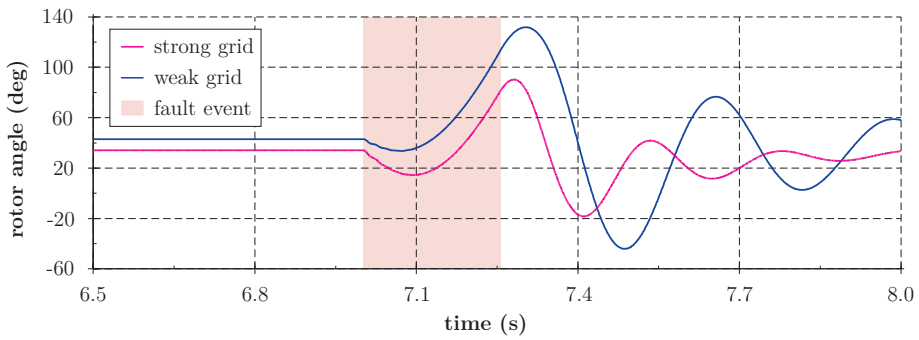

Figure 5.4: Generator rotor angle excursions in a weak and a strong grid

5.3 Influence of LVRT Test Equipment on the Dynamic Performance of a Power Generation Unit

The capability of power generation units to withstand a defined voltage-against-time-profile, the so-called LVRT capability, has to be proven by type testing or unit testing (see subsection 4.4), before they are allowed to be connected to the grid. In order to verify the LVRT capability of a power generation unit (PGU), it either has to be tested on-site with certain test equipment or simulations using a validated simulation model of the power generation unit have to be performed. The most common way to test power generation units is using a test container[8], which is emulating a fault event in the grid with reduced short circuit power. Thus this subsection focuses on this test equipment's influence on the dynamic performance of a power generation unit, which applies for both simulation and on-site tests. This setup is mostly referred to as LVRT test container and therefore, will also be called by that term henceforth.

Simulations with different setups with and without LVRT test container and variation of the fault location, but always keeping the same short circuit ratio and remaining voltage at the power generation unit's connection point, reveal different transient behavior of the device under test.

5.3.1 Case Study

A simulation model has been set up, using an EMT simulation method, which is more appropriate in that case than RMS methods[9]. Simulation results are going to show the influence of an LVRT test container on the dynamic performance of a power generation unit when facing a fault event. The simulation model of the synchronous machine including

[8] Other test methods see subsection 4.2 "Case Study".

[9] For further details on RMS and EMT simulation methods see subsection 6.2.2.

a voltage regulator and excitation system with all relevant limiters has been verified through measurements by an accredited certifier, as discussed in subsection 4.4.

5.3.2 Simulation Setup

The configuration used for simulation is the same as introduced in subsection 5.2 above. It basically consists of a gas engine driven synchronous generator (data see Table 5.1), connected via cable to the low voltage side of the transformer (data see Table 5.2), which finally connects to the external MV grid via another cable.

To achieve a worst case scenario for rotor angle excursions, the operating point of the synchronous machine is set to full load at pf=0.95 under-excited. In terms of the backswing phenomenon (see subsection 6.2), an operating point at light machine loading with an over-excited power factor is the most severe one. Since the backswing is not the most demanding case for most setups, results for over-excited operating points are not shown here. The voltage dip was set according to ENTSO-E requirements [4] to a remaining voltage of u=0.05 pu and a duration of t=250 ms. The dip depth is adjusted by changing the value of the shunt impedance without the PGU connected.

The advantage of setting the remaining voltage with the power generation unit disconnected is that the resulting voltage divider is independent of the generator and therefore easy to determine and to set up. The disadvantage is that the actual remaining voltage during test runs can be quite different and hard to determine beforehand, because it depends on the transient response of the power generation unit during the fault event. When setting up the test equipment to adjust the remaining voltage with the EUT connected, the remaining voltage will obviously be the same for all kinds of tests and generators, as the voltage would be set individually. The big disadvantage in that method is that it is difficult to account for the transient behavior of the EUT connected in advance, in order to predict the remaining voltage during the fault. Hence, the test equipment settings will have to be adjusted in an iterative process to accomplish a certain remaining voltage with the EUT connected.

A test procedure utilized in Spain sets the remaining voltage depending on the SCR. If SCR<5, then the remaining voltage is set with the EUT connected. Otherwise it is set with the EUT disconnected, because the influence of the transient response of the EUT is negligible at higher SCRs. This procedure has the advantage that it delivers almost the same remaining voltages throughout different tests, but also simplifies the setup for tests with SCR 5. [48]

Following, three scenarios are defined to demonstrate the influence of the test equipment and choice of the fault location.

Scenario 1:

Between the power generation unit and the transformer, a LVRT test container is introduced, as illustrated in Figure 5.5. Short circuit power S_k" of the supplying is fixed with S_k"=263.1 MVA. The series impedance Z_1 of the test container is adjusted to achieve a certain short circuit power ratio at the generator terminals. In order to assure proper LVRT capability of the PGU in weak grids as well, short circuit power ratios are usually given by standards or technical guidelines like FGW [49] in the range of $S_k"/P_r$=3…5. In this case a ratio of $S_k"/P_r$=3.5 was chosen. This corresponds to a test container series impedance of 14 Ω (X/R=20). The series impedance Z_1 is already activated at the beginning of the simulation. The short circuit impedance Z_2 is set to 0.82 Ω (X/R=20).

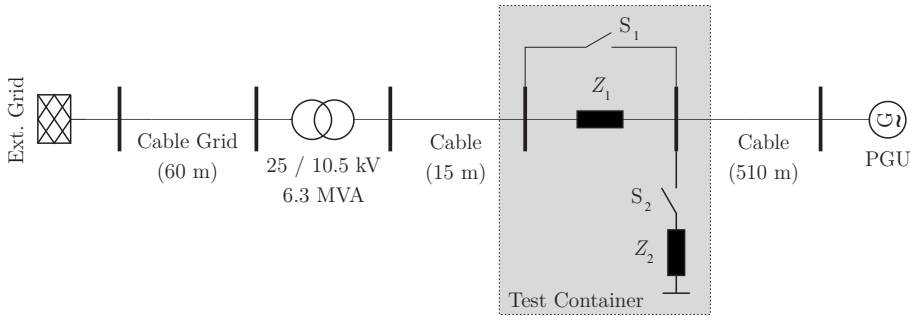

Figure 5.5: Test setup scenario 1

Scenario 2:

To compare the results with the test container to a setup without a test container, the short circuit power of the supplying grid has to be adjusted, to achieve the same short circuit power ratio at generator terminals. In this case this means reducing the short circuit power down to S_k"=8.4 MVA. In Figure 5.6 the grid setup for this scenario is shown. As can be seen, the short circuit event is still created by switching an impedance for the desired fault time of 250 ms. In this case, the short circuit impedance has to be 0.76 Ω (X/R=20).

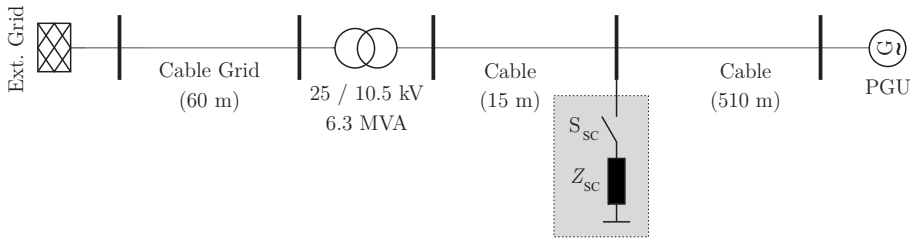

Figure 5.6: Test setup scenario 2

Scenario 3:

Additionally a third scenario is defined. Same settings as defined in scenario 2 apply, only that the fault location has been changed from the PCC to the external grid's busbar. With it the value of the short circuit impedance has to be changed as well, in order to achieve the same voltage dip depth at generator terminals. Now it has to have an impedance of 3.94 Ω (X/R=20). The grid setup for this scenario is shown in Figure 5.7.

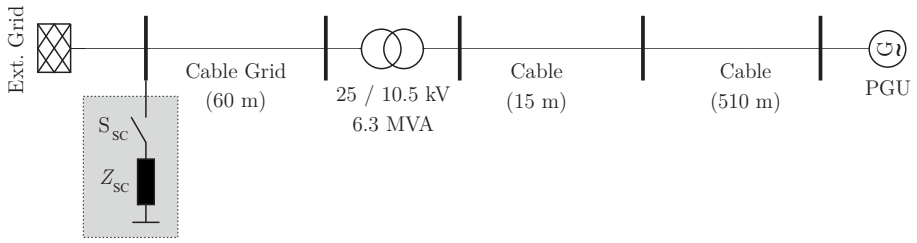

Figure 5.7: Test setup scenario 3

5.3.3 Simulation Results

The main difference between results with and without a test container lies in the fact that the series impedance of the test container, which in this case is quite big compared to grid impedances, causes a significant voltage drop. This is visualized in Figure 5.8, which shows the voltage profile along the network elements between the external grid and the PGU. In contrast, voltage drop between the external grid and the PGU is considerable low without a test container, which is shown in Figure 5.9. The voltage profile for scenario 3 is the same as for scenario 2 and therefore not shown explicitly.

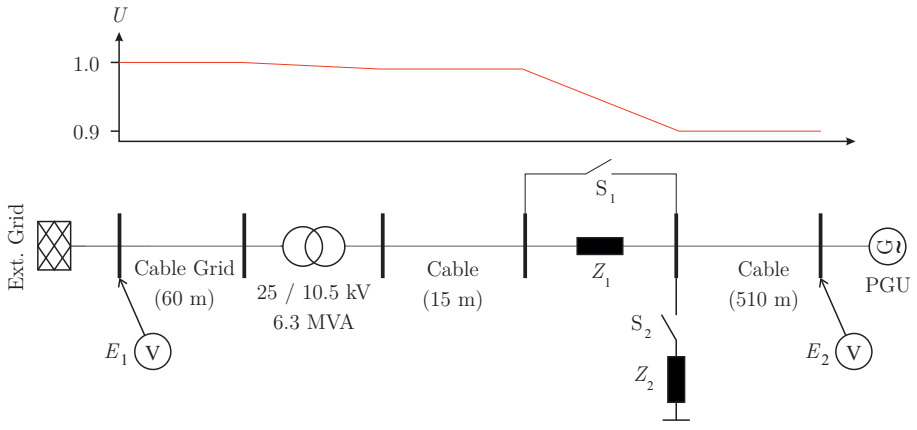

Figure 5.8: Voltages in test setup scenario 1

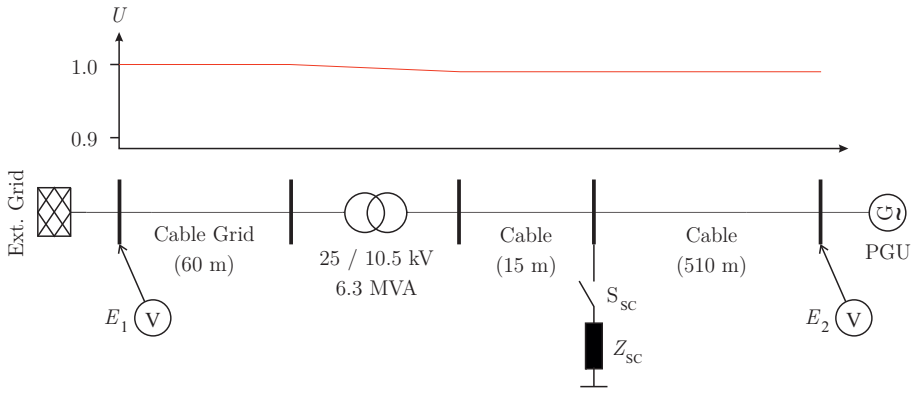

Figure 5.9: Voltages in test setup scenario 2

If one assumes same operating points in both scenarios, the stationary rotor angle in scenario 1 has to be higher due to the lower voltage E_2 at generator terminals, in order to achieve the same power flow P_{12}, which can be approximated by equation (5.4).

$$P_{12} = \frac{E_1 E_2}{Z_T} \cdot \sin\left(\vartheta_1 - \vartheta_2\right) \tag{5.4}$$

Where Z_T is the total grid impedance, E_1 the external grid voltage, E_2 the PGU voltage, ϑ_1 the external grid reference angle and ϑ_2 the generator rotor angle. Besides, in scenario 1 the retarding power in the first few cycles is not as big as in scenario 2. This is because the lower voltage at generator terminals in scenario 1 causes a lower initial short circuit current and therefore, a weaker backswing effect (see subsection 6.2). Another disadvantage in scenario 1 presents the lower synchronizing torque due to the higher initial rotor angle.

Rotor angles of the three defined scenarios are shown in Figure 5.10. As can be seen the performance of the machine is different in those cases, although the same remaining voltage and the same short circuit power at generator terminals are defined.

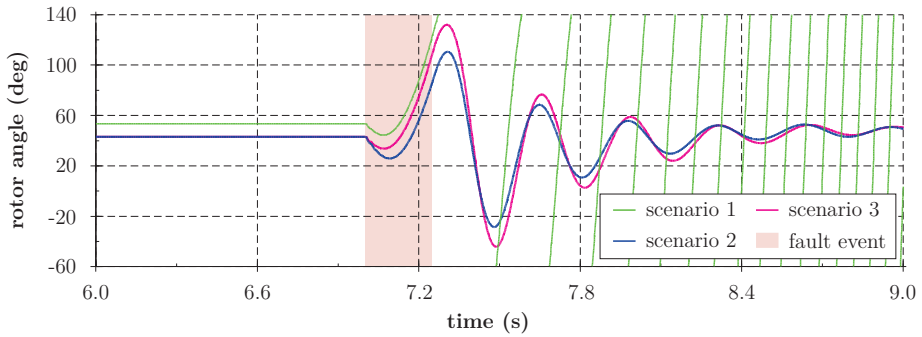

Figure 5.10: Generator rotor angle excursions for scenario 1, 2 and 3

5.4 Conclusion

A case study demonstrated how varying the SCR can impact the dynamic behavior of a synchronous generator by examining the transient excursions of rotor angle and active power, in addition to the generator terminal voltage. It has been shown, that varying the short circuit power of the external grid does not only alter the steady state rotor angle, but also the dynamic behavior of the synchronous machine when facing a fault event. Equations have been given to describe how external parameters like the short circuit impedance can affect the magnitude and frequency of oscillations, when facing a fault event.

It's also been shown that an LVRT test container can have a significant influence on the dynamic performance of a power generation unit. Depending on the short circuit power of the grid the EUT is connected to, the influence of the container is more or less severe. Given a strong grid, where the short circuit power is high, the series impedance of the test container has to be set to a relatively high value, in order to achieve a certain low short circuit ratio at the PCC. Hence, the effect on the dynamic performance is more pronounced. On the other hand, if the short circuit power of the grid is already low, there's no need for a huge series impedance to significantly reduce the short circuit ratio and therefore, influence of the test container is lower. Although the IEC 61400-21 (see subsection 4.3) states, that the series impedance should not affect the transient response at the terminals, no specific values or calculation methods are mentioned. As can be seen in Figure 5.10, the performance of the EUT is different in each scenario, although facing the same remaining voltage and short circuit power. Hence, using an LVRT test container might lead to an evaluation being too restrictive.

The method of setting the remaining voltage during a fault with the EUT disconnected has the disadvantage, that the actual remaining voltage with the PGU connected is on the one hand higher than set and on the other hand depending on fault location and generator operating point. Nonetheless, this is common practice and has the advantage that the voltage dip depth doesn't have to be adjusted for different scenarios or different machines. Besides, setting the actual remaining voltage during a fault event to a specific value can be quite challenging as already stated.

One simple solution to reduce the influence of an LVRT test container would be to adapt the tap changer positions of the transformer, in order to adjust the PGU terminal voltage. This way the results are very similar to the ones without a test container, assuming same fault event, short circuit ratio and generator terminal voltage prior to the fault event.

6 LVRT Capability Improvement

Extensive research is being done on grid codes and LVRT-requirements. Iov et al.[30], Tsili and Papathanassiou [50] and Sourkounis and Tourou [51] investigate and compare different grid codes and their requirements and operating limits regarding frequency, voltage, power factor and active and reactive power control. Grid codes are mostly compiled by transmission system operators (TSOs) of countries or regions with high penetration of regenerative energy sources. A lot of research work has been done for the improvement of LVRT-behavior of wind farms, especially for doubly-fed induction generators [52, 53].

Especially for engines with low inertia, the acceleration of the rotor during a fault event is very critical and can lead to loss of synchronism of the machine. This section focuses on means to improve the LVRT capability of power generation units. Such equipment can help the machine to ride through faults, i.e. keeping synchronism with the external grid without disconnecting. A retardation device is presented, which is able to curtail the acceleration during fault events to keep synchronism of the generator with the external grid and thereby be grid code compliant. The examined retardation device is a switchable ohmic resistance, which is connected in series to the generator. All simulations are performed with the power system analysis software DIgSILENT PowerFactory.

6.1 Introduction

During fault events in the electrical power grid nearby a synchronous generator, the rotor speed of the machine is increased, because of the imbalance between the mechanical power fed to the generator and the electrical power fed to the grid. This may cause high generator rotor angle excursions and hence the machine to lose synchronism with the power grid.

There have been approaches to face those requirements and help generators ride through a fault without losing synchronism. Some of the most common mitigation methods are:

- **Series braking resistor:**
  Ohmic resistor in series to the power generation unit to increase dissipated power by introducing additional ohmic losses.
- **Parallel braking resistor:**
  Ohmic resistor in parallel to the power generation unit to increase dissipated power by introducing additional ohmic losses.
- **Full power converter:**
  The power generation unit can be decoupled from the grid – and with it from faults in the grid – by using a full power converter.

- **Eddy-current brake:**
  Rotor speed increase during a fault is slowed down by activating an eddy-current brake.
- **Flywheel mass:**
  Mitigating rotor angle excursions by increasing the total inertia by means of installing additional flywheel mass.
- **Control strategy:**
  Mostly relevant for inverter based generation and DFIG based generation, where the LVRT behavior is mainly determined by the inverter's control strategy.
  For conventional power generation units, AVR tuning can help in reducing rotor angle excursions, although the impact is usually quite limited. For gas engine driven power generation units, ignition or misfire control are reasonable means to reduce the turbine power input to the generator and with it the power imbalance during a fault event.

All of these solutions come with certain advantages and disadvantages. Tröster and Krieger [54] give a brief overview of the different solutions and comparing their characteristics, such as functionality, costs, efficiency and market availability.

Although the backswing effect – which will be examined in the following subsection – decelerates the rotor (more or less, depending on the test setup), in most cases acceleration of the rotor due to lack of dissipated and transferred power during a fault event is dominating, which can cause the machine to lose synchronism. To prevent the machine from falling out of step, a retardation device must be introduced. One way to do so is to increase the dissipated power during a fault by introducing an impedance in series to the generator. To increase dissipated real power, the series impedance has to be basically ohmic. As the problem of lacking power dissipation only persists during fault, the series resistor is activated upon detection of a fault event only and bypassed otherwise.

6.2 Backswing Phenomenon

Considering a generator during fault, typically an imbalance between mechanical power from the engine and electrical power fed to the grid emerges, leading to acceleration or deceleration of the rotor and possible loss of synchronism. Two basic effects can occur: The first and obvious one is the acceleration of the rotor due to reduced electrical torque during the voltage drop. However, in some cases a deceleration in the first cycles of the fault can be observed – the backswing.

Although the backswing very often is neglected in transient performance studies, taking it into account can be quite important. Depending on the test setup and operating point of the machine, the backswing effect can have a quite significant impact on active power output and accordingly on rotor speed and rotor angle. However, the backswing effect can be advantageous to the generators transient stability too, because it allows more time to clear a fault. Both the oscillatory and the unidirectional torque components have to be accounted for to achieve satisfying results for electrical torques and with it rotor angle. The lower the pre-fault power level, the more severe the backswing. The larger the reactances of the grid near the machine, the higher the excitation level needs to be and with that, terminal voltage is higher. As a result, air-gap flux is higher and therefore, if a short circuit occurs, the initial transient losses and the initial unidirectional torque are increased. In addition to the factors pre-fault load and excitation level, the backswing is more severe if inertia is decreased or when the fault is closer to the machine, which causes a higher short circuit current and losses. The duration of the backswing is affected by armature resistance and field- and damper-winding time constants [55, 56].

The backswing effect can be explained as follows: After a short circuit, the flux wave represented by flux linkages of d- and q-axis, Ψ_d and Ψ_q, respectively, remains as flux wave stationary referred to the armature. Therefore, voltages are induced in the rotor circuits and the consequent currents cause power losses in the ohmic resistances of the rotor. These losses, combined with armature short circuit power losses, produce a unidirectional braking torque, which is counteracting the engine's torque. Hence, the backswing is decelerating the rotor and therefore, helping the machine ride through the fault. Nevertheless, in some cases this effect might be too strong and therefore, contribute to instability. Besides the unidirectional torque, the oscillatory torque components, which are of fundamental and double-fundamental frequency, influence the backswing as well. These components add up to the total post-fault torque. In Figure 6.1 exemplary results of the measured rotor angle excursions of a short circuit on a 56 MVA generator and simulation results of rotor angle excursions neglecting the backswing effect are shown. It is evident, that this backswing phenomenon has a significant influence on the dynamic behavior of the machine. It must be noted thought, that the influence of the backswing effect heavily depends on a lot of factors, as elaborated in more detail later. So for another setup, the backswing might not be as severe as shown here, but just as likely even more pronounced.

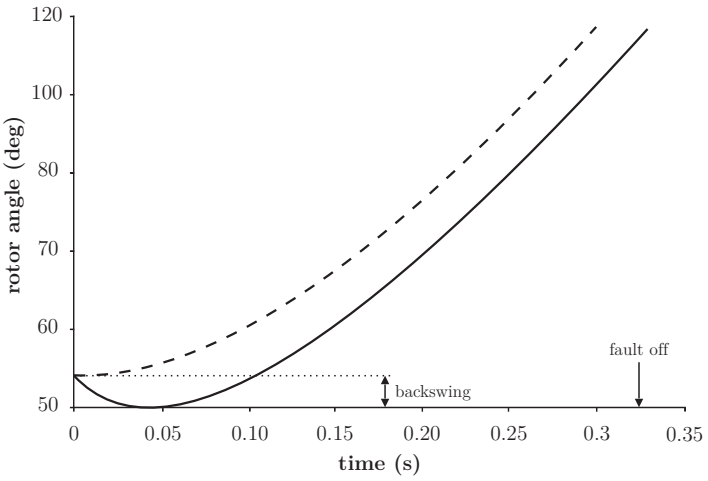

Figure 6.1: Rotor angle test curve vs. simulation results (neglecting backswing) [56]

The total electrical torque T_e contains oscillating terms, at angular frequencies ω and 2ω, and unidirectional terms, which depend on the resistances and are of smaller magnitude than the oscillating terms. The oscillatory torques of fundamental frequency arise as a result of an exchange of energy from the kinetic energy of the rotor to magnetic energy of the generator. [55]

The formula for the electrical torque T_e is given in equation (6.1) with a few simplifications and assumptions given by Mehta and Adkins [1].

$$\begin{aligned} T_e = \frac{1}{2}\cdot\Big\{ & \Big[v_{q0}\cdot\left(i_{d0}+i_{dt}\right)-v_{d0}\cdot\left(i_{q0}-i_{qt}\right)\Big]\cdot e^{-\alpha t}\sin\omega t-\Big[v_{d0}\cdot\left(i_{d0}+i_{dt}\right)+v_{q0}\cdot\left(i_{q0}-i_{qt}\right)\Big]\cdot e^{-\alpha t}\cos\omega t \\ & +\frac{1}{2}\cdot\left(v_{q0}^2-v_{d0}^2\right)\cdot\left(\frac{1}{X_q''}-\frac{1}{X_d''}\right)\cdot e^{-2\alpha t}\sin 2\omega t-v_{q0}\cdot v_{d0}\cdot\left(\frac{1}{X_q''}-\frac{1}{X_d''}\right)\cdot e^{-2\alpha t}\cos 2\omega t \\ & +r_a\cdot\left[\left(i_{d0}+i_{dt}\right)^2+\left(i_{q0}-i_{qt}\right)^2\right] \\ & +\frac{1}{2}\cdot\left(v_{q0}^2+v_{d0}^2\right)\cdot\left(\frac{R_{d1}}{X_d'^2}+\frac{R_{d2}}{X_d''^2}+\frac{R_q}{X_q''^2}\right)\cdot e^{-2\alpha t} \\ & +\frac{1}{4}\cdot\left(v_{q0}^2+v_{d0}^2\right)\cdot\left(\frac{1}{X_d''}-\frac{1}{X_q''}\right)^2\cdot r_a\cdot e^{-2\alpha t}\Big\} \end{aligned} \tag{6.1}$$

Equation (6.1) can be divided into five components. Each line of the equation is represented by one of the following components, adequately numbered corresponding to the line in the equation [57]:

1. A fundamental-frequency component depending on the direct-axis sub-transient reactance.

2. A double-frequency component depending on the sub-transient saliency[10].
3. A unidirectional component of torque proportional to the stator i^2r losses, where i is the AC component of the stator current with fundamental frequency, hence representing the armature winding copper losses.
4. A unidirectional component of torque proportional to the rotor i^2r losses, where i is the AC component of the rotor current or the DC component of the stator current. This component represents the copper losses due to the induced currents of fundamental frequency in the field and damper circuits.
5. A unidirectional component of torque due to the sub-transient saliency[10].

Unfortunately, equation (6.1) doesn't allow for all the losses occurring after a short circuit. Specifically the damper losses due to currents at supply frequency are increased because of eddy currents in the bars and in the core. Therefore, the unidirectional torque component due to rotor i^2r losses is increased. [1]

Literature by Shackshaft [55] focuses on the oscillating terms, rather than the unidirectional terms, since, according to his studies, they can have a significant influence as well, although they are often times neglected in other literature.

6.2.1 Case Study

The backswing phenomenon describes the behavior of a synchronous generator in the first cycle(s) of the fault, where dissipated power is slightly higher than the driving mechanical power input, compared to the operating point prior to the fault. Therefore, the rotor is decelerated before being accelerated. This behavior is shown in Figure 6.2, where simulation results for a synchronous machine's active power output P are shown. The machine used for simulation was a 2.492 MVA synchronous generator (data see Table 5.1 in subsection 5.2) running at full load and pf=0.95 ind. The simulated fault was a voltage dip to u=0.05 pu at the point of common connection (PCC) for 250 ms (highlighted red area). The generator's rotor angle excursions are displayed in Figure 6.3. It shows the decline of the rotor angle within the first few cycles due to the backswing effect before its first peak due to rotor acceleration.

[10] Sub-transient saliency is the difference between x_{q}" and x_{q}".

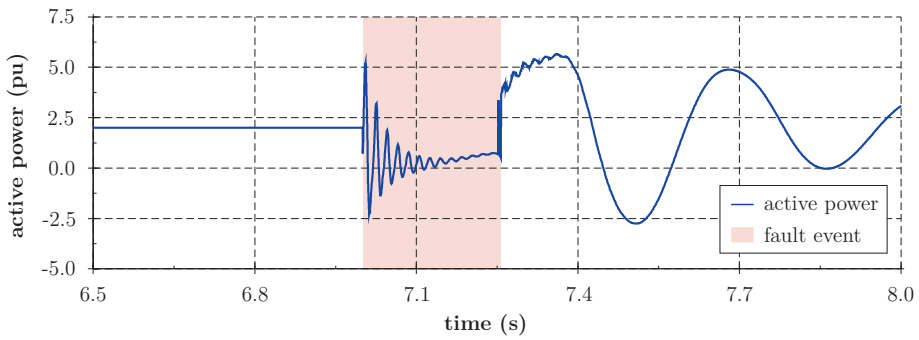

Figure 6.2: Active power output capturing the backswing effect

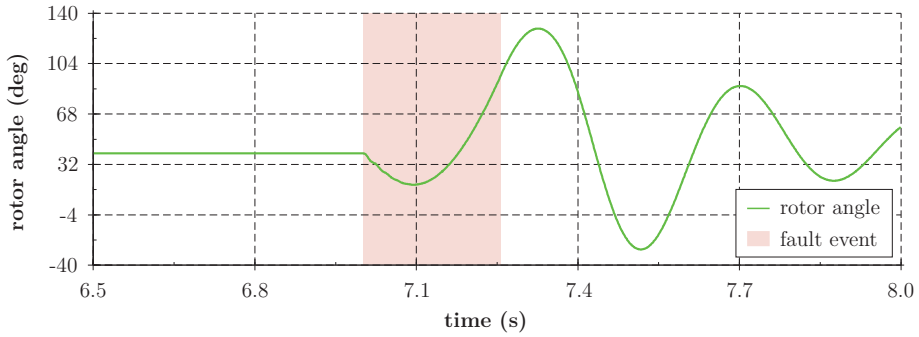

Figure 6.3: Rotor angle excursion due to backswing effect

6.2.2 Simulation Methods

As already briefly introduced in the literature survey in subsection 2.3, there are basically two dynamic simulation methods available in power system analysis programs: the instantaneous value simulation (EMT – Electro-Magnetic Transients) and the transient stability simulation (RMS – Root Mean Square). In EMT-simulations, the machine's flux and stator voltage equations are represented without simplifications. Therefore, dc components as well as harmonic components in short circuit currents and generator torque are represented in simulation results. In contrast, using the RMS simulation method, the machine's stator voltage equations get simplified (stator flux transients neglected).

The advantage of an RMS simulation is that the simulation time is significantly reduced compared to an EMT simulation. The increased simulation speed makes it possible to simulate much longer events and much more complex systems. Figure 6.4 shows exemplary simulation results of active power during and after facing a fault event (highlighted in red) lasting 150 ms, using the RMS and EMT simulation method. [25]

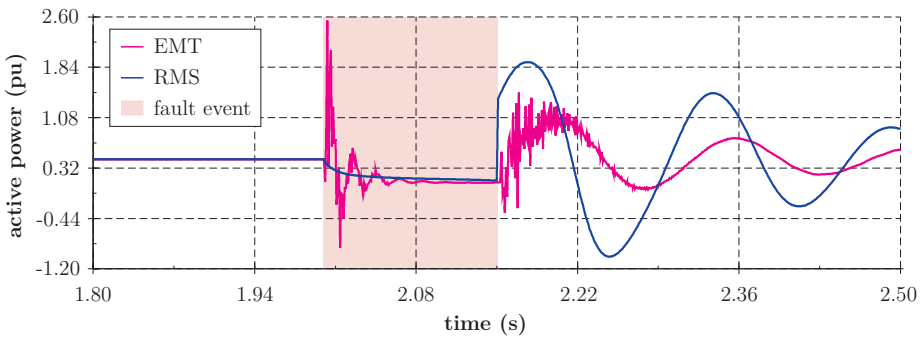

Figure 6.4: Synchronous generator active power output during fault event using the EMT and RMS simulation method

As can be seen, high-frequency power oscillations are not represented using the RMS-simulation-method, whereas using the EMT-simulation method, high-frequency components are represented properly. So in order to properly show the effect of the backswing phenomenon in simulations, the EMT simulation method should be used.

6.3 Series Resistor Design

The engaging of a series resistance inserted between generator and grid will lead to increased I^2R-losses during fault. Since the short circuit current depends on the remaining voltage during the dip, the series resistor solution shows an inherent self-stabilizing behavior. A lower remaining voltage leads to a higher power imbalance for the synchronous machine. However, it also causes a larger short circuit current and a larger power dissipated in the resistor, mitigating the power imbalance. Besides the series resistor, the ohmic parts of the components in the power supply of the generator must be taken into account. This is especially important in low-voltage installations with a low X/R-ratio.

In steady state conditions, there's a balance between the turbine power input P_{T} and the generator's electrical power output P_{gen} fed to grid (neglecting power conversion losses), which can be approximated by equation (6.2), where U_1 is the generator's inner voltage, U_2 the voltage of the external grid and ϑ the angle between the two voltages. X_{t} is the sum of reactances between the generator and the external grid.

$$P_{gen} = \frac{U_1 \cdot U_2}{X_t} \cdot \sin \vartheta \tag{6.2}$$

In case of a fault event, the balance between turbine power and generator output power is disturbed. During the fault, the generated power P_{gen} fed to the grid can be significantly lower compared to its pre-fault value, because of the change in total reactance X_{t} and voltage U_2, which now equals the remaining voltage at the fault location. This unbalance of active power can be reduced by increasing ohmic losses caused by the generator's short

circuit current I_{SC}, which can be expressed in a good approximation with equation (6.3), as given in IEEE Standard 1110-1991 for synchronous generator modeling in stability studies [23].

$$I_{SC} = \frac{E}{X_{du}} + \left(\frac{E}{X'_d} - \frac{E}{X_{du}} \right) \cdot e^{-t/T'_d} + \left(\frac{E}{X''_d} - \frac{E}{X'_d} \right) \cdot e^{-t/T''_d} \tag{6.3}$$

Here, E is the machine's inner voltage and U_{ret} the remaining voltage at the fault location. Equation (6.3) assumes that the fault location is at the generator terminals. Considering a distant fault, impedances between the fault location and the generator terminals have to be taken into account as well. Furthermore, resistances and the remaining voltage at the fault location is considered also, which results equation (6.4):

$$\begin{aligned} I_{SC} = (E - U_{ret}) \cdot \Bigg(& \frac{1}{\sqrt{X_{du}^2 + R^2}} + \left(\frac{1}{\sqrt{X_d'^2 + R^2}} - \frac{1}{\sqrt{X_{du}^2 + R^2}} \right) \cdot e^{-t/T'_d} \\ & + \left(\frac{1}{\sqrt{X_d''^2 + R^2}} - \frac{1}{\sqrt{X_d'^2 + R^2}} \right) \cdot e^{-t/T''_d} \Bigg) \end{aligned} \tag{6.4}$$

This equation can be further simplified by approximating the time-dependent terms. This simplification given in equation (6.5) yields satisfying results for an average value of the fault current during a given fault time duration t_f, which has been verified through simulations. Including the fault duration t_f considers the share of transient and sub-transient components on the average fault current $I_{SC,avg}$.

$$\begin{aligned} I_{SC,avg} = (E - U_{ret}) \cdot \Bigg(& \frac{1}{\sqrt{X_{du}^2 + R^2}} + \left(\frac{1}{\sqrt{X_d'^2 + R^2}} - \frac{1}{\sqrt{X_{du}^2 + R^2}} \right) \cdot \frac{T'_d}{t_f} \\ & + \left(\frac{1}{\sqrt{X_d''^2 + R^2}} - \frac{1}{\sqrt{X_d'^2 + R^2}} \right) \cdot \frac{T''_d}{t_f} \Bigg) \end{aligned} \tag{6.5}$$

With that, the dissipated power P_V due to I^2R losses in the sum of all ohmic resistances between the generator and the fault location is:

$$P_V = I_{SC,avg}{}^2 \cdot R \tag{6.6}$$

The active power P'_{gen} fed to grid during the fault can be approximated as follows:

$$P'_{gen} = \frac{E \cdot U_{ret}}{X} \cdot \sin \vartheta_0 \tag{6.7}$$

The difference of both voltages E and U_{ret} is driving the fault current I_{SC}. Impedance X and resistance R are the sum of all reactances and resistances, respectively, between the fault location and the generator. ϑ_0 is the initial value of the rotor angle at the beginning of the

fault event. In reality, the rotor angle ϑ would change throughout the duration of the fault, but is assumed to be constant, which is sufficient to give a rough approximation of the active power P'_{gen} fed to the external grid.

Another part of the active power balance equation is determined by the backswing effect. Though often neglected, it has shown to have a significant influence on the dynamic behavior of synchronous machines, as discussed in subsection 6.2. The contribution of the backswing phenomenon on the total electrical torque is given in equation (6.1). Mehta and Adkins [1] have shown that the dominant part is the unidirectional component of torque $T_{\mathrm{e,4}}$ proportional to the rotor I^2R losses, which is shown in equation (6.8):

$$T_{e,4} = \frac{1}{4} \cdot \left(v_{q0}^2 + v_{d0}^2 \right) \cdot \left(\frac{R_{d1}}{X_d'^2} + \frac{R_{d2}}{X_d''^2} + \frac{R_q}{X_q''^2} \right) \cdot e^{-2\alpha t} \tag{6.8}$$

Here, R_{d1} is the field winding resistance (d-axis) and R_{d2} and R_{q} are the damper winding resistances in d- and q-axis. They can be calculated from the time constants T_{d}', T_{d}" and T_{q}". Kundur [22] gives the following equations for calculation R_{d1}, R_{d2} and R_{q}:

$$\left.\begin{aligned} T_d' &\approx \frac{1}{R_{d1}} \cdot \left(L_{fd} + \frac{L_{ad} \cdot L_l}{L_{ad} + L_l} \right) \\ L_d' &= L_l + \frac{L_{ad} \cdot L_{fd}}{L_{ad} + L_{fd}} \approx L_{fd} + \frac{L_{ad} \cdot L_l}{L_{ad} + L_l} \end{aligned}\right\} \rightarrow R_{d1} \approx \frac{L_d'}{T_d'}$$

$$\left.\begin{aligned} T_d'' &\approx \frac{1}{R_{d2}} \cdot \left(L_{1d} + \frac{L_{ad} \cdot L_{fd} \cdot L_l}{L_{ad} \cdot L_l + L_{ad} \cdot L_{fd} + L_{fd} \cdot L_l} \right) \\ L_d'' &= L_l + \frac{L_{ad} \cdot L_{fd} \cdot L_{1d}}{L_{ad} \cdot L_{fd} + L_{ad} \cdot L_{1d} + L_{fd} \cdot L_{1d}} \approx L_{1d} + \frac{L_{ad} \cdot L_{fd} \cdot L_l}{L_{ad} \cdot L_l + L_{ad} \cdot L_{fd} + L_{fd} \cdot L_l} \end{aligned}\right\} \rightarrow R_{d2} \approx \frac{L_d''}{T_d''} \tag{6.9}$$

$$\left.\begin{aligned} T_q'' &\approx \frac{1}{R_q} \cdot \left(L_{1q} + \frac{L_{aq} \cdot L_{2q} \cdot L_l}{L_{aq} \cdot L_l + L_{aq} \cdot L_{2q} + L_{2q} \cdot L_l} \right) \\ L_q'' &= L_l + \frac{L_{aq} \cdot L_{1q} \cdot L_{2q}}{L_{aq} \cdot L_{1q} + L_{aq} \cdot L_{2q} + L_{1q} \cdot L_{2q}} \approx L_{1q} + \frac{L_{aq} \cdot L_{2q} \cdot L_l}{L_{aq} \cdot L_l + L_{aq} \cdot L_{2q} + L_{2q} \cdot L_l} \end{aligned}\right\} \rightarrow R_q \approx \frac{L_q''}{T_q''}$$

For speeds around nominal frequency the electrical torque $T_{\mathrm{e,4}}$ can be assumed to be equal to the electrical power P_{BS}, which is given in equation (6.10), along with some simplifications.

$$\begin{aligned}
&\left(v_{q0}^2 + v_{d0}^2\right) \approx \left(E - U_{ret}\right)^2 \\
&e^{-2\alpha t} = e^{-2t/T_a} \\
&P_{BS} = \underbrace{\frac{1}{4} \cdot \left(E - U_{ret}\right)^2 \cdot \left(\frac{1}{X'_d \cdot T'_d \cdot \omega_0} + \frac{1}{X''_d \cdot T''_d \cdot \omega_0} + \frac{1}{X''_q \cdot T''_q \cdot \omega_0} \right) \cdot CF}_{P_{BS\max}} \cdot e^{-2t/T_a}
\end{aligned} \tag{6.10}$$

The correction factor CF accounts for two aspects: Even though the unidirectional component of torque $T_{e,4}$ due to the rotor I^2R losses is the biggest contributor to the backswing torque in equation (6.1), the other four components have a share as well. But even when considering the other parts as well, Mehta and Adkins [1] found out that not all losses are accounted for. Therefore, the correction factor CF is introduced. Since the backswing effect is a function of the pre-fault loading level of the generator as well, this correlation is considered by including the pre-fault rotor angle ϑ into the correction factor. Various simulations of different setups and generators have shown that a correction factor of around $CF = 2 \cdot \cos \vartheta_0$ gives satisfying results for the backswing representation.

The armature time constant T_a can be calculated with equation (6.11)[11].

$$T_a = \frac{1}{r_a} \cdot \left(\frac{X''_d + X''_q}{2} \right) \tag{6.11}$$

Ideally, putting all these equations together, a balance can be found between the generator turbine power input P_t, the power output P'_{gen} fed to the external grid, the retarding power P_{BS} due to the backswing phenomenon and the losses P_V in ohmic resistances, which leads to equation (6.12):

$$P_t - P'_{gen} - P_V - P_{BS} = 0 \tag{6.12}$$

Since the backswing retarding power P_{BS} is still a function of time, the following approach has been taken. Instead of examining the power balance, a balance in energy is considered. Because the backswing phenomenon is only present in the very first part of a fault[12], the following assumption is valid:

$$\lim_{t \to t_f} e^{-2t/T_a} \approx \frac{T_a}{2} \tag{6.13}$$

[11] This equation applies for short circuits at generator terminals, but is sufficient as an approximation in this case.

[12] Considering fault durations in the range of 100-250 ms.

All other active power quantities given in equation (6.12) are assumed to be constant and therefore, are present during the whole fault duration t_f. This leads to the final equation for the energy balance given by equation (6.14).

$$P_t \cdot t_f - P'_{gen} \cdot t_f - P_V \cdot t_f - P_{BS\max} \cdot \frac{T_a}{2} = 0 \tag{6.14}$$

This equation can then be solved for the total ohmic resistance R. Since it's a quadratic function of R, there are two results $R_{1,2}$, as illustrated in Figure 6.5. In reality, the smaller value might be the more practicable solution.

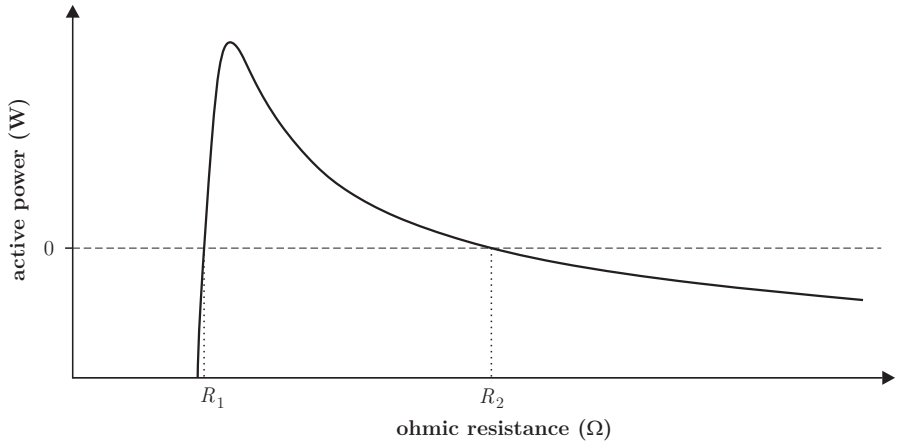

Figure 6.5: Power equilibrium as a function of total ohmic resistance R

It has to be noted, that the resistances $R_{1,2}$ represent the total ohmic resistances between the generator and the fault location, including a series resistor. So in order to calculate the actual value of the series resistor, resistances of cables, transformers, generator and fault location have to be subtracted from $R_{1,2}$. Another import remark is, that the calculations had to be based on some approximations, otherwise it won't be feasible to replace complex dynamic computer simulations by simple equations. This means that the calculated value of a series resistor as a retardation device based on the given equations, is not an exact one. In some scenarios the results might be very close to a theoretically optimal value, but in others they might be a bit off. But the idea is to get a rough estimation of the approximate value of a braking resistor, rather than to get an exact value, which is not necessary to help the machine ride through a fault.

For the calculation of the series resistor a power balance, or rather energy balance, has been assumed. But if an equilibrium during the fault can't be reached exactly, this doesn't necessarily mean that the synchronous machine loses synchronism and disconnects. A certain disturbance is always tolerated by the machine. So usually it's not a single resistor value but a certain range, which meets the desired stability criteria, such as no loss of

synchronism or keeping the rotor angle or rotor speed in a certain range around their nominal operating point.

The series resistor value is determined as follows: The operating point is set to maximum power, the remaining voltage at the PCC is set to u=0.05 pu, the dip duration according to ENTSO-E requirements [4] to t=250 ms and the circuit breaker activation delay to 25 ms (see subsection 6.4). In an iterative process the value of the series resistor at a certain remaining voltage level is increased from zero until the stability criteria (no loss of synchronism, limited rotor angle deviation or limited speed deviation) is reached. This resistor value is the lower limit of the possible range. Then the resistor value is further increased until the range of stable LVRT is left again, marking the upper value of the possible resistor range. In a next step the remaining voltage is increased and the process repeated. Again the result is a range for the resistor value. Due to the self-stabilizing effect described above, the determined resistor ranges will clearly overlap. So it is possible to determine a single value which covers different remaining voltages, respectively identify the voltage limit where stability is kept without series resistor. After that, the simulation is extended to operation points below maximum power, using the predetermined resistor value. In some scenarios it will happen, that the power dissipation of the resistor is too high. In those cases, the on-time of the resistor will be reduced. Simulation has shown that the on-time of the resistor can be easily controlled according to the loading of the machine. For simulation results regarding resistor dimensioning see Table 6.3 in subsection 6.5.2.

6.4 Control Strategy

The series resistor should be activated after the backswing effect has decayed, because otherwise the activation of the braking system would intensify the backswing effect. By then, the conventional problem of low generator power can be approached with engaging the series resistance. However, when the backswing has decayed, the braking system should get activated as soon as possible to maximize the braking effect. The activation delay of the system is an essential parameter to define its effectiveness.

Anyway, from a practical point of view, an instantaneous activation of the series resistance is not possible. Referring to realistic activation times, including fault detection (15 ms) and commutation delay (5 ms), thyristor-controlled elements should be able to activate the series resistor within 25 ms. This value is used for the simulations. The thyristor has to be in parallel to the series resistor to build a bypass for the operational current during normal operation. Thyristor controlled switches are chosen over common LV circuit breakers, since the response time of the latter is in the range of 60 ms. The system loses its effectiveness by further delaying the activation. Depending on the delay, the rotor acceleration may be too progressed to stop over-speeding. Consequently, a fast reaction

ensures efficiency and operational ranges of the braking system in the same way as an optimal designed resistor does.

The series resistance is deactivated when the fault is cleared (respecting detection and commutation delays), or earlier if necessary. Therefore, depending on the loading of the machine and the remaining voltage during fault, the series resistor is activated or not.

6.5 Case Study

The simulations were performed in power system analysis software DIgSILENT PowerFactory, using the EMT simulation method. The simulation model of the synchronous machine including a voltage regulator and limiters has been verified through measurements (see section 4.4 for further details).

6.5.1 Simulation Setup

The setup used for simulation was a small low voltage grid as shown in Figure 6.6. It basically consists of a gas engine driven generator (data see Table 6.1), connected via cables and the series resistor to the low voltage side of the transformer (data see Table 6.2) and finally via another cable to the external power grid. The breaker element represents the thyristor controlled switch. The red flash depicts the location, where the fault event is set – in this case the PCC. P1 and P2 are active power measurement points used for illustration of series resistor action in the simulation results (see Figure 6.11 in subsection 6.5.2).

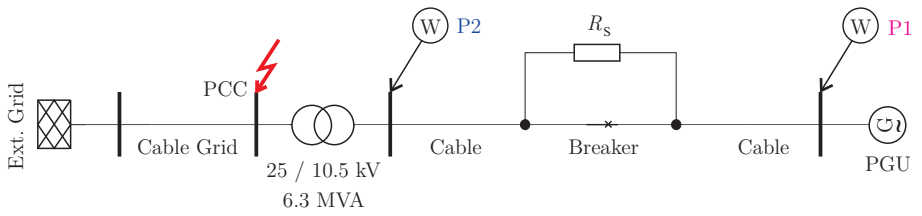

Figure 6.6: Grid setup for simulations

To achieve a worst case scenario for rotor angle excursions, the operating point of the generator is set to pf=0.95 under-excited. Loading of the machine is varied from no load to full load. Short circuit power S_k" of the external grid was set to 20 MVA. Following, generator and transformer data are shown in Table 6.1 and Table 6.2, respectively.

Table 6.1: Generator data

Parameter	Value	Unit
U_n	0.4	kV
S_n	792	kVA
H	0.32	MWs/MVA
x_d	2.173	pu
x_q	1.628	pu
x_d‘	0.161	pu
x_d‘‘	0.128	pu
x_q‘‘	0.14	pu
T_d’	0.156	s
T_d’’	0.010	s
T_q’’	0.012	s

Table 6.2: Transformer data

Parameter	Value	Unit
U_{n1}	25	kV
U_{n2}	0.4	kV
S_n	1.6	MVA
u_k	5.5	%
P_{cu}	16	kW
I_0	1.3	%

6.5.2 Simulation Results

In Table 6.3 the results of the series resistor dimensioning process (see subsection 6.3) are given. Green shaded areas indicate ranges where no activation of the series resistor is necessary, orange shaded areas indicate a limited on-time (here: 55 ms) of the resistor and yellow shaded areas indicate operation of the series resistor during the whole duration of the voltage dip. As can be seen in Table 6.3, it is possible to use the same ohmic resistance for all investigated cases for the given setup. Ohmic resistances of cables, transformer and generator between the fault location and the generator total 6.34 mΩ.

Table 6.3: Series resistor dimensioning

Load	Voltage at PCC				
	0%	5%	10%	20%	30%
0%					
10%					
20%					
30%					
40%					
50%					
60%					
70%	30 mΩ 55ms	30 mΩ 55ms	30 mΩ 55ms		
80%	30 mΩ 55ms	30 mΩ 55ms	30 mΩ 55ms	30 mΩ 55ms	
90%	30 mΩ	30 mΩ	30 mΩ	30 mΩ	30 mΩ
100%	30 mΩ	30 mΩ	30 mΩ	30 mΩ	30 mΩ

Following, simulation results performing a voltage dip are shown for two specific simulation setups selected from Table 6.3. Results for rotor angle, rotor speed and active power at terminals P1 and P2 are shown. The difference between active power at P1 and P2 during fault illustrates the action of the series resistance. Data for the first simulation setup is shown in Table 6.4.

Table 6.4: Simulation setup 1

Parameter	Value	Unit
Residual voltage U_{PCC}	0.05	pu
Machine loading P_{Load}	0.9	pu
Series resistance R_{S}	30	mΩ
Time of fault	2	s
Fault duration	0.25	s
Activation delay of R_{S}	0.025	s
Activation time of R_{S}	2.025	s
Deactivation time of R_{S}	2.275	s
Maximum rotor angle	±120	°

Figure 6.7 shows the generator rotor angle without activation of series resistance R_{S}. It can be seen that the generator falls out of step at about t=2.2 s. The red area highlights the fault event. Fortunately, in this case the generator is able to gain synchronism with the grid again. Nevertheless, such a behavior is undesired under any circumstances.

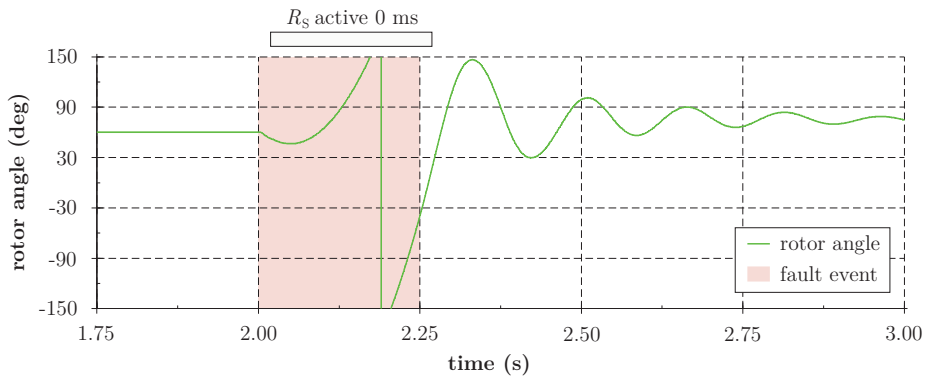

Figure 6.7: Generator rotor angle without activation of series resistance R_S (setup 1)

Following, generator rotor speed without activation of series resistor R_S is shown in Figure 6.8. In this specific case, the rotor speed is able to get back to its pre-fault level after the pole-slip as well.

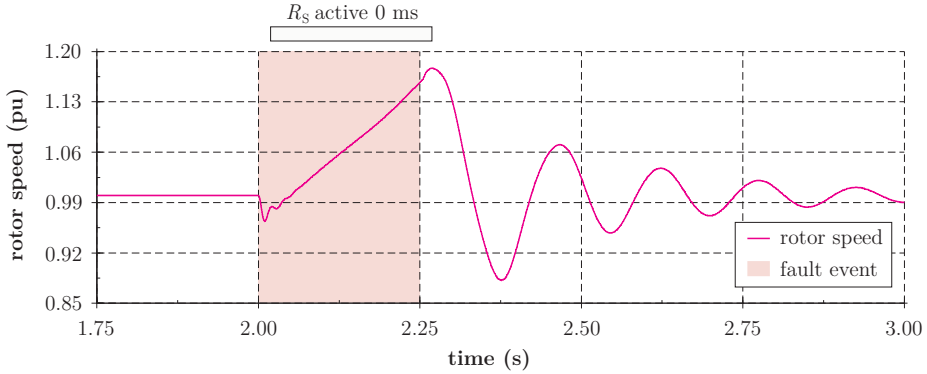

Figure 6.8: Generator rotor speed without activation of series resistance R_S (setup 1)

Figure 6.9, Figure 6.10 and Figure 6.11 show the rotor angle, rotor speed and active power measurements, respectively, with operation of the series resistor. The blue bar above each graph shows the duration of activation of the series resistance R_S.

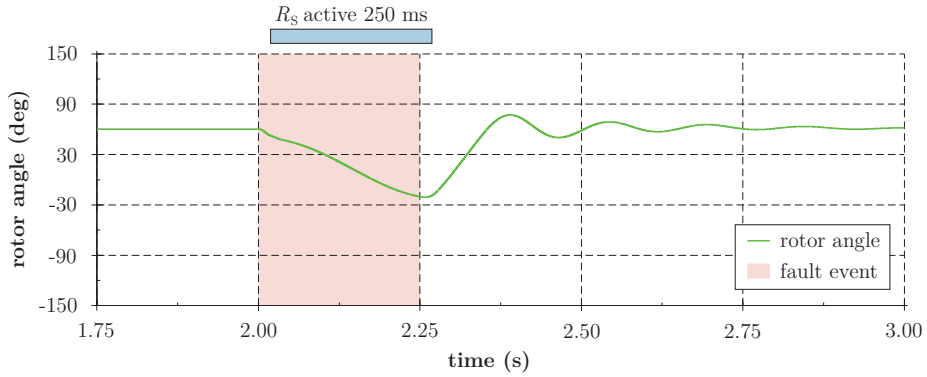

Figure 6.9: Generator rotor angle with activation of series resistance R_S (setup 1)

It can be seen that rotor angle excursions are limited to an acceptable level and can be kept within the set boundaries.

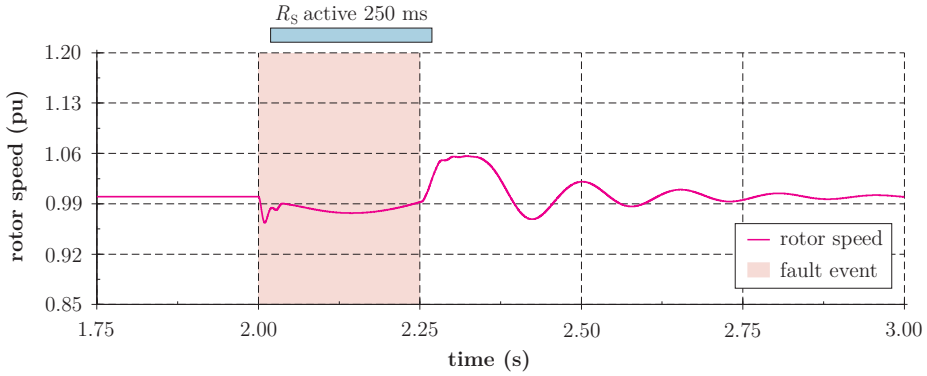

Figure 6.10: Generator rotor speed with activation of series resistance R_S (setup 1)

From Figure 6.10 one can see how the series resistance R_S is not only preventing the acceleration of the rotor, but also stabilizing it on a certain level during activation time of the resistor.

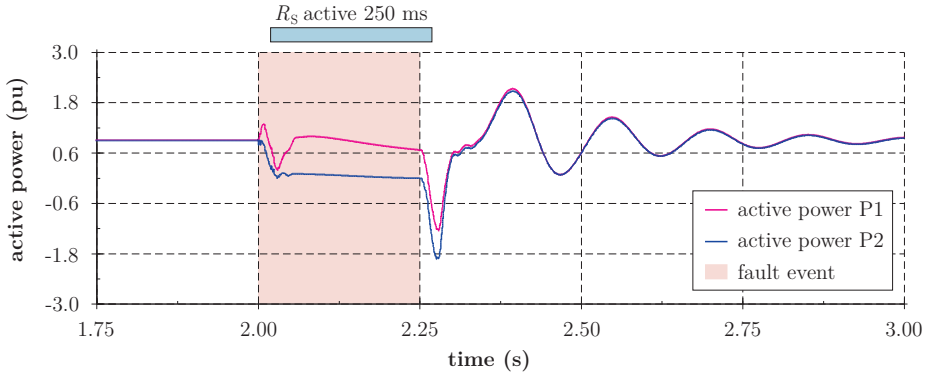

Figure 6.11: Active power measurements at terminals P1 and P2 with activation of series resistance R_S (setup 1)

Drawing attention to the difference between active power signals at P1 and P2, one can clearly see the action of the series resistor. The area between both signals during fault mainly corresponds to the series resistors dissipated energy. A considerable difference between active power at P1 and P2 within the period of fault start and activation of R_S can be seen, because the initial short circuit current (sub-transient part) is very high and therefore, the active power dissipated in the cables between the two measurement points P1 and P2 is noticeable.

The second simulation setup is shown in Table 6.5. In this case, the series resistor is not active the whole time during fault, but only for 55 ms.

Table 6.5: Simulation setup 2

Parameter	**Value**	**Unit**
Residual voltage U_{PCC}	0.05	pu
Machine loading P_{Load}	0.7	pu
Series resistance R_S	30	mΩ
Time of fault	2	s
Fault duration	0.25	s
Activation delay of R_S	0.025	s
Activation time of R_S	2.025	s
Deactivation time of R_S	2.080	s
Maximum rotor angle	±120	°

Following, plots for generator rotor angle and rotor speed without activation of R_S are shown in Figure 6.12 and Figure 6.13, respectively.

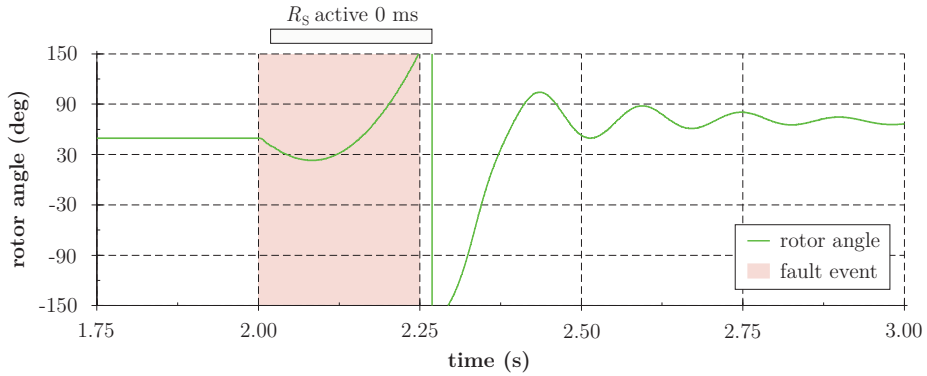

Figure 6.12: Generator rotor angle without activation of series resistance R_S (setup 2)

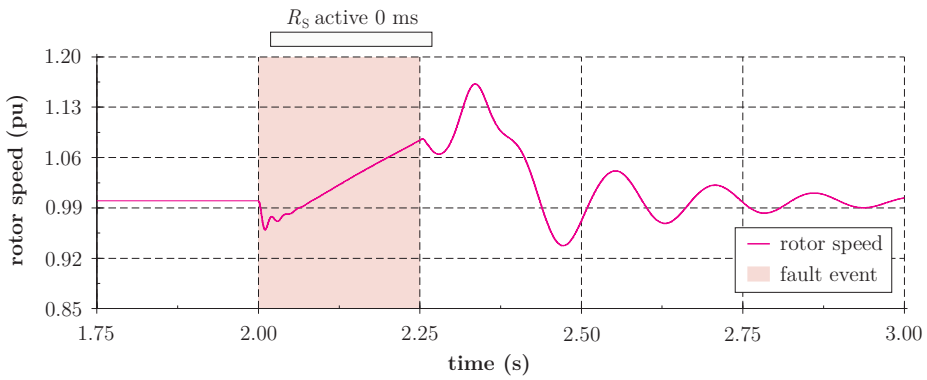

Figure 6.13: Generator rotor speed without activation of R_S (setup 2)

Results for rotor angle, rotor speed and active power with activation of the series resistance R_S for a limited time (here 55 ms) are shown in Figure 6.14, Figure 6.15 and Figure 6.16, respectively.

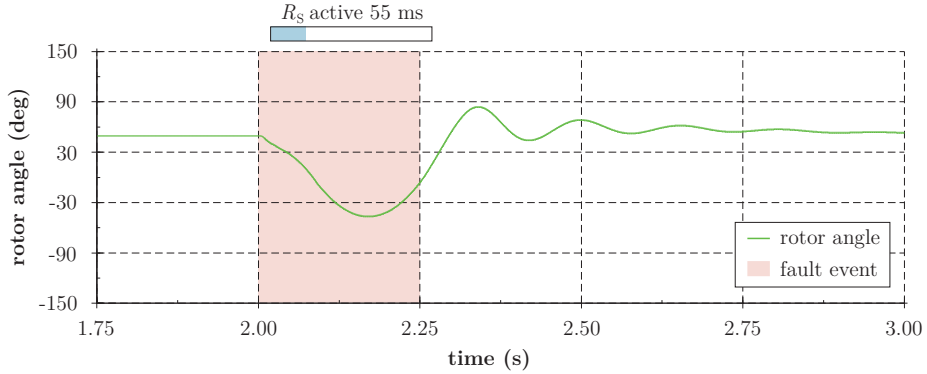

Figure 6.14: Generator rotor angle with activation of series resistance R_S for 55 ms (setup 2)

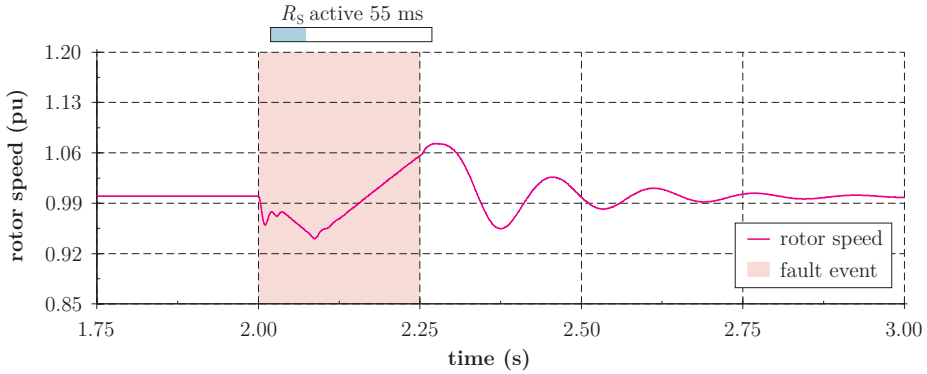

Figure 6.15: Generator rotor speed with activation of series resistance R_S for 55 ms (setup 2)

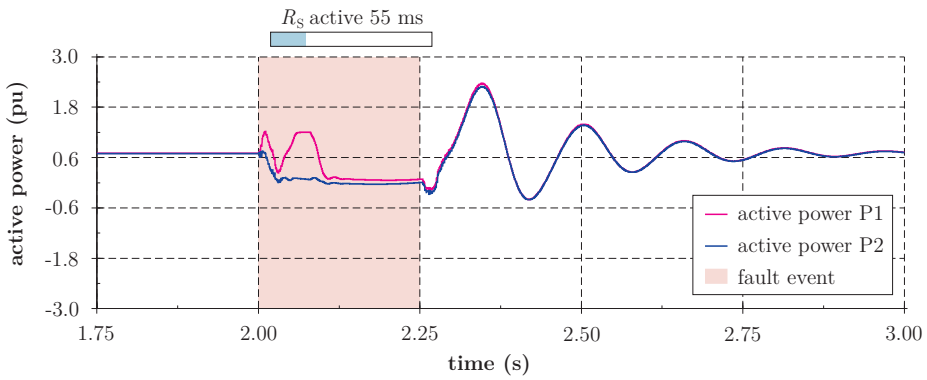

Figure 6.16: Active power measurements at terminals P1 and P2 with activation of series resistance R_S for 55 ms (setup 2)

It can be clearly seen in Figure 6.15, that if the series resistor would have been activated the whole time during fault, the generator would have decelerated too far. This is because dissipated power in the series resistor is almost the same as in the first simulation setup, but this time the pre-fault active power operation point is lower. Therefore, activation of R_S leads to a power output higher than the power input of the generator, which leads to deceleration and can be seen in Figure 6.16.

6.6 Conclusion

The backswing phenomenon has been introduced. It's an often neglected detail in the transient behavior of synchronous machines. Its retarding power within the first cycles of a fault can have a significant impact on the LVRT behavior of a machine. It has been shown, that it's mandatory to use the EMT simulation method to properly reproduce the backswing effect in simulations. Especially for the dimensioning of a series breaking resistor as a retardation device, it is important to account for the backswing effect as well. Approximation guidelines are given on how to consider the backswing analytically.

A retardation device was introduced into a low voltage grid setup to reduce rotor acceleration during fault and with it prevent losing synchronism of the generator with the grid. Different machine sets and grid topologies were simulated. The simulation results have shown that introducing a switchable series resistance to the grid setup is able to keep all selected values within its boundaries and therefore, prevent generator rotor slip. Series braking resistor dimensioning guidelines have been formulated, assuming an energy equilibrium during the fault event.

One of the big advantages of the series resistance as a retardation device is the simplicity of its control and the inherent self-stabilizing behavior. Besides that, no changes to the mechanical structure or the drive train are necessary. On the negative side are permanent

losses in normal operation mode of the thyristor modules, because they have to carry the operational current in continuous duty.

On-site tests and simulations have shown that not only rotor angle or rotor speed excursions can cause generators to disconnect from the grid during fault events, but also protection devices, such as stator current and excitation current limiters. Therefore, the ability to ride through a fault without disconnecting from the grid is not only a matter of keeping the rotor angle in check, but also minding the operation of protective devices.

7 Conclusion and Outlook

Motivated by the emerging of grid codes and with it a variety of LVRT requirements applicable to power generation units, important topics regarding these requirements have been investigated. One of the most referred LVRT requirements are LVRT profiles, defining what kind of voltage dips the power generation unit has to be able to withstand, without disconnecting from the power grid. As regarded in the first research question, the speculation was that those LVRT requirements might be too strict. An investigation of fault statistics and voltage dip statistics of several different countries or regions has shown similar results, namely that severely low voltages – as demanded by most LVRT profiles – are very rare. The same conclusion was drawn from performing simulations on a Central European power grid. Voltage sag propagation analyses have shown, that severely low voltages are confined to small areas and therefore, do not affect a significant amount of power generation or compromise system frequency stability. This has been shown for worst case scenarios, utilizing bolted 3-phase short circuits. In reality, those do rarely occur, so the effects of faults would be even less severe.

Another issue that arises more often when conducting such investigations, is the question of how the performance of a future grid might look like, when conventional generation is to a certain degree replaced with renewable energy sources. With the largest share being wind power plants and photovoltaics, the short circuit power is decreased, since those are inverter based generation units mostly. Such a reduction in short circuit power has been taken into account by reducing the short circuit power of all generation in the Central European power grid. Results have shown, that even reducing it down to 10 % of the original short circuit power, the average short circuit power at the substations throughout the grid doesn't change as drastically. Therefore, the remaining voltages when performing short circuit simulations do not change by much either. This means that the conclusion for a power grid with a lot of inverter based generation is essentially the same: Voltages below u=0.2 pu are locally confined and therefore, only a few power plants would face serious low voltages that could endanger proper operation of their units. Regarding research question 1, whether LVRT requirements are too strict or justified, it has been shown that LVRT profiles are too demanding. Therefore, it might be reasonable to loosen the requirements, especially for smaller generation units.

If a power generation unit needs to be connected to a certain power grid, it has to adhere to the relevant grid code and with it LVRT requirements. This LVRT capability can be proven through certain tests, as has been shown. Depending on the test method applied, certain limitations are present. A detailed investigation of the influence of an LVRT test container on the dynamic behavior of a power generation unit has shown, that depending on the grid setup, the impact of the test equipment can be quite significant, since no specific

instructions are given in technical guidelines regarding on-site testing. Fortunately, in case of the LVRT test container, simply adjusting the voltage tap changer positions of the transformer between the machine and the external grid, can mitigate the impact of the test equipment significantly. So regarding research question 2, it can be stated that state-of-the-art LVRT test procedures by means of an LVRT test container are reasonable, if its possible impacts are considered and countermeasures taken, when necessary.

Research question 3 concerns LVRT validation procedure and its methods, significant parameters and limitations. The validation procedure, as is customary in Germany when applying for an LVRT certificate by validating simulation models, was introduced and scrutinized. Technical guidelines define how measurements have to be taken, how to evaluate them and how simulation models are validated. The timeline of an LVRT test has to be divided into certain areas. Each area has to have a transient and a stationary part. For each area and transient or stationary part, certain error margins have to be kept according to the technical guidelines. This comes with the problem that some areas of certain setups show transient behavior only, but still a stationary part has to be defined within this area. Obviously, adhering to given error margins in simulation results becomes challenging. Aside from certain obstacles by technical guidelines, modeling of the excitation system and AVR is just as challenging as parameterizing the model. However parameterizing the controller isn't a big deal, once the model structure is set, since it's a digital controller and therefore, the parameter set of the real controller can be used in simulations as well. What's more challenging is fine-tuning data, which comes with tolerances, such as machine and saturation data. According to generator manufacturers, machine parameters come with tolerances up to 40 %.

As already mentioned previously, some power generation units – especially smaller ones with low inertia – might have problems riding through faults defined in LVRT requirements. Addressing research question 4, different methods aiding power generations with keeping rotor angle and speed excursions in check have been shown. The focus in this thesis was put on a series braking resistor as a retardation device. Its functionality has been shown in a case study. The series resistor dimensioning was elaborated in detail. The key factors in determining the resistor value were accounting for the backswing effect and the approximation of the short circuit current. Neglecting the backswing phenomenon, the share of dissipated power by I^2R losses gets overestimated, and with it the braking resistor value. The average short circuit current over the duration of the fault was not approximated by a sub-transient or transient impedance behind a constant voltage source, because this yielded inaccurate results. An equation was derived, where the average short circuit current is a function of transient and sub-transient impedances, transient and sub-transient time constants and fault duration. But still, this analytical expression of the series resistor dimensioning is only an approximation and therefore not able to replace complex

dynamic simulations. This means that the given equations provide an estimate of the series braking resistor, rather than to pinpoint its value.

Regarding future work in this field of research it might be interesting to investigate how different grid structures can have an impact on issues like voltage sag propagation. That could be power grids with longer connection lines in between substations, as currently the case in wider areas of America or Canada for example. Relating possible future power grids, utilizing HVDC back-to-back interconnections of certain areas or HVDC interconnection lines will result in new challenges and research questions, since the implementation of such equipment alters the behavior of a power grid, e.g. by reducing its short circuit power to a certain degree. Since grid codes often times do also mention LVRT requirements regarding active and reactive power fed to the grid by a power generation unit when facing a fault event, investigations should be made, how the majority of future power generation – like wind power plants or photovoltaics – is able to cope with such requirements or system ancillary services in general. Furthermore, it is highly recommended to consider research and statistics when formulating or updating LVRT requirements in grid codes

8 References

[1] D. B. Mehta and B. Adkins, “Transient torque and load angle of a synchronous generator following several types of system disturbance,” *Proceedings of the IEE Part A: Power Engineering*, vol. 107, no. 31, pp. 61–74, http://ieeexplore.ieee.org/stamp/stamp.jsp?arnumber=5242435, 1960.

[2] N. P. Traian, U. Kjetil, and E. N. r. Dag, “An overview of the present grid codes for integration of distributed generation,” in *Integration of Renewables into the Distribution Grid, CIRED 2012 Workshop*, 2012, pp. 1–4.

[3] A. Q. Al-Shetwi, M. Z. Sujod, and N. L. Ramli, “A review of the fault ride through requirements in different grid codes concerning penetration of PV system to the electric power network,” *ARPN Journal of Engineering and Applied Sciences*, vol. 10, no. 21, pp. 9906–9912, 2015.

[4] Official Journal of the European Union, *Establishing a network code on requirements for grid connection of generators*. Brussels, Belgium, 2016.

[5] ENTSO-E, *Implementation Guideline for Network Code "Requirements for Grid Connection Applicable to all Generators".*

[6] S. Probert, *Generator Fault Ride Through (FRT) Investigation: Literature Review.*

[7] ENTSO-E, *Justification of the FRT-Requirement for Type B Units in the RfG Network Code: Meeting with DSO Technical Expert Group.*

[8] ENTSO-E, *Network Code on "Requirements for Generators": Evaluation of Comments.*

[9] P. W. Christensen, *Grid Codes The Manufacturer's Nightmare*. Warsaw, 2010.

[10] ENTSO-E, *Network Code for Requirements for Grid Connection Applicable to all Generators: Frequently Asked Questions.*

[11] Bollen, Math H. J, *IEEE tutorial on voltage sag analysis*. Gothenburg, Sweden: Chalmers University of Technology, 1999.

[12] M. T. Aung and J. V. Milanović, “Analytical assessment of the effects of voltage sags on induction motor dynamic responses,” in *2005 IEEE Russia Power Tech*, 2005.

[13] M. T. Aung, J. V. Milanović, and S. C. Vegunta, “The Influence of Induction Motors on Voltage Sag Propagation—Part I: Accounting for the Change in Sag Characteristics,” *Power Delivery, IEEE Transactions on*, vol. 23, no. 2, pp. 1063–1071, http://ieeexplore.ieee.org/stamp/stamp.jsp?arnumber=4454202, 2008.

[14] WGTF, "The Technical Basis for the New WECC Votlage Ride-Through (VRT) Standard," 2007.

[15] N. C. Nair and W. A. Qureshi, "Systematic development of Low Voltage Ride-Through (LVRT) envelope for grids," in *IEEE Region 10 Annual International Conference, Proceedings/TENCON*, 2010, pp. 574–579.

[16] N.-K. C. Nair and W. A. Qureshi, "Fault Ride-Through Criteria Development," in *Green Energy and Technology*, Singapore, 2014, pp. 41–67.

[17] A. Eliasson and E. Isabegovič, *Modeling and simulation of transient fault response at Lillgrund Wind Farm when subjected to faults in the connecting 130 kV grid*. Göteborg: Chalmers University of Technology, 2009.

[18] CIGRE, *Voltage Dip Immunity of Equipment and Installations: Working Group C4.110*. Paris: CIGRÉ, 2010.

[19] M. Östman, N. Wägar, I. Ristolainen, and J. Klimstra, *The impact of grid dynamics on low voltage ride through capabilities of generators.*

[20] ENTSO-E, *Network Code for Requirements for Grid Connection Applicable to all Generators: Requirements in the Context of Present Practices.*

[21] C. Abbey and G. Joos, "Effect of low voltage ride through (LVRT) characteristic on voltage stability," in *2005 IEEE Power Engineering Society General Meeting*, 2005, pp. 1901–1907.

[22] P. Kundur, *Power system stability and control*. New York: McGraw-Hill, 1994.

[23] IEEE, "IEEE Guide for Synchronous Generator Modeling Practices in Stability Analyses," *IEEE Std 1110 1991*, 1991.

[24] WECC, *Specification of the Second Generation Generic Models for Wind Turbine Generators*, 2014.

[25] P. E. Sørensen *et al., Simulation and verification of transient events in large wind power installations.*

[26] E. Ortjohann *et al.,* "A Dynamic-RMS modeling method for distributed generation," in *2009 IEEE Power & Energy Society General Meeting*, 2009, pp. 1–8.

[27] FGW, *Technical Guidelines for Power Generating Units: Part 4*. Demands on Modelling and Validating Simulation Models of the Electrical Characteristics of Power Generating Units and Systems

[28] J. Ahnlund, *Short-circuit contributions from fully-rated converter wind turbines: Modeling and simulation of steady-state short-circuit contribution from FRC wind turbines in offshore wind power plants*. Stockholm, Sweden: KTH Royal Institute of Technology, 2014.

[29] DIgSILENT, *DIgSILENT PowerFactory User Manual: Version 15.* Gomaringen, Germany: DIgSILENT GmbH, 2015.

[30] F. Iov, A. D. Hansen, P. Sørensen, and N. A. Cutululis, *Mapping of grid faults and grid codes.* Roskilde, Denmark: DTU Risø National Laboratory, 2007.

[31] M. Fontela, S. Bacha, N. Hadjsaid, and C. Andrieu, *Functional Specifications of electric Networks with high degrees of distributed generation: Distributed Intelligence in Critical Infrastructures for Sustainable Power.*

[32] ENTSO-E, *Nordic and Baltic Grid Disturbance Statistics 2014.*

[33] P. Heine and M. Lehtonen, "Voltage sag distributions caused by power system faults," *IEEE Transactions on Power Systems*, vol. 18, no. 4, pp. 1367–1373, http://ieeexplore.ieee.org/stamp/stamp.jsp?arnumber=1245559, 2003.

[34] D. S. Dorr *et al.,* "Interpreting recent power quality surveys to define the electrical environment," *Conference Record - IAS Annual Meeting (IEEE Industry Applications Society)*, vol. 4, pp. 2251–2258, 1996.

[35] CEER, *5th CEER Benchmarking Report on the Quality of Electricity Supply 2011.*

[36] E. A. Mertens *et al.,* "Evaluation and trends of power quality indices in distribution system," in *2007 9th International Conference on Electrical Power Quality and Utilisation, EPQU*, 2007.

[37] M. Diaz, R. Cardenas, and G. Soto, "4-wire Matrix Converter based voltage sag/swell generator to test LVRT in renewable energy systems," in *Ecological Vehicles and Renewable Energies (EVER) 2014 Ninth International Conference on*, 2014, pp. 1–10.

[38] C. Wessels, R. Lohde, and F. W. Fuchs, "Transformer based voltage sag generator to perform LVRT and HVRT tests in the laboratory," in *2010 14th International Power Electronics and Motion Control Conference (EPE/PEMC)*, 2010, T11-8-T11-13.

[39] IEC, *International standard IEC 61400-21: Wind turbines - Part 21: Measurement and assessment of power quality characteristics of grid connected wind turbines,* 2nd ed. Geneva: International Electrotechnical Commission, 2008.

[40] M. García-Gracia, M. Paz Comech, J. Sallán, D. López-Andía, and Ó. M. Alonso, "Voltage dip generator for wind energy systems up to 5 MW," *Applied Energy*, vol. 86, no. 4, pp. 565–574, 2009.

[41] C. Veganzones *et al.,* "Voltage dip generator for testing wind turbines connected to electrical networks," *Renewable Energy*, vol. 36, no. 5, pp. 1588–1594, 2011.

[42] FGW e.V., *Zertifizierung der Elektrischen Eigenschaften von Erzeugungseinheiten und -anlagen am Mittel-, Hoch- und Höchstspannungsnetz,* 6th ed. Berlin: Fördergesellschaft Windenergie und andere Erneuerbare Energien, 2013.

[43] BDEW, *Generating Plants Connected to the Medium-Voltage Network: Guideline for generating plants' connection to and parallel operation with the medium-voltage network,* 2008th ed. Frankfurt, M., Berlin, Heidelberg: VWEW-Energieverl., 2008.

[44] BDEW, *Rules and transition periods for specific requirements in addition to the Technical Guideline: Generating Plants Connected to the Medium-Voltage Network - Guideline for Generating Plants' Connection to and Parallel Operation with the Medium-Voltage Network.*

[45] J. Langstädtler, *Netzanschluss: Nachweisverfahren und Zertifizierung: Aktuelle Anforderungen und Erfüllung der gültiger [sic] Regelwerke.*

[46] IEEE, *IEEE Recommended Practice for Excitation System Models for Power System Stability Studies.* [Place of publication not identified]: [publisher not identified], 2006.

[47] J. Machowski, J. W. Bialek, and J. R. Bumby, *Power system dynamics: Stability and control,* 2nd ed. Chichester, U.K.: Wiley, 2008.

[48] AEE, *Procedure for Verification Validation and Certification of the Requirements of the Po 12.3 on the Response of Wind Farms and Photovoltaic Plants in the Event of Voltage Dips.*

[49] FGW, *Technical Guidelines for Power Generating Units: Part 3.* Determination of electrical characteristics of power generating units connected to MV, HV and EHV grids

[50] M. Tsili and S. Papathanassiou, "A review of grid code technical requirements for wind farms," *Renewable Power Generation, IET*, vol. 3, no. 3, pp. 308–332, http://ieeexplore.ieee.org/stamp/stamp.jsp?arnumber=5237667, 2009.

[51] C. Sourkounis and P. Tourou, *Grid Code Requirements for Wind Power Integration in Europe.*

[52] A. Yunus, A. Abu Siada, and M. Masoum, "Improvement of LVRT capability of variable speed wind turbine generators using SMES unit," in *2011 IEEE PES Innovative Smart Grid Technologies Asia (ISGT)*, 2011, pp. 1–7.

[53] K. T. Aung and H. Saitoh, "Pitch control for improving the low-voltage ride-through of wind farm," in *Transmission & Distribution Conference & Exposition: Asia and Pacific, 2009*, 2009, pp. 1–4.

[54] E. Tröster and G. Krieger, *Comparison of different Fault-Ride-Through solutions for gas engine power plants based on simulations.*

[55] G. Shackshaft, *Effect of oscillatory torques on the movement of generator rotors.*

[56] R. G. Harley and B. Adkins, *Calculation of the angular back swing following a short circuit of a loaded alternator.*

[57] C. Concordia, *Synchronous machines: Theory and performance*. New York: Wiley, 1951.